Title

Bacterial lag phase shortening is triggered by methyl groups

Authors/affiliations:
Martin Sperfeld[1†], Delia A. Narváez-Barragán[1†], Sergey Malitsky[2], Veronica Frydman[3], Lilach Yuda[1], Jorge Rocha[4], Einat Segev[1*]

[1]Department of Plant and Environmental Sciences, Weizmann Institute of Science, Rehovot 7610001, Israel
[2]Department of Life Sciences Core Facilities, Weizmann Institute of Science, Rehovot 7610001, Israel
[3]Department of Chemical Research Support, Weizmann Institute of Science, Rehovot 7610001, Israel
[4]Conacyt- Unidad Regional Hidalgo, Centro de Investigación en Alimentación y Desarrollo, San Agustín Tlaxiaca 42162, Mexico

Author list footnotes:
[†]authors contributed equally
*corresponding author and lead contact

Corresponding author e-mail address:
einat.segev@weizmann.ac.il

Summary

Short lag times are beneficial for heterotrophic bacteria that compete for resources in environments with fluctuating organic carbon levels. We found that the marine model bacterium *Phaeobacter inhibens* achieves shorter lag times in the presence of nano- to micromolar concentrations of *N*- or *S*-methylated compounds, which are abundantly produced by microalgae. To understand the underlying mechanism, we studied algal-bacterial co-cultures and bacterial pure cultures during their lag phase using transcriptomics analyses, ^{13}C-labeled metabolomics, gene knock-out experiments and enzymatic characterizations. Our findings highlight methyl group synthesis as a bottleneck during the bacterial lag phase, which can be overcome by assimilating methyl groups from external sources. Our study reveals a fundamental aspect of the bacterial lag phase, emphasizing the importance of studying bacterial physiology within an ecological framework, particularly in the context of microbial interactions.

Highlights

- Methylated compounds are a resource that induces bacterial lag phase shortening.
- The beneficial effect arises from the assimilation of methyl groups.
- Methyl group assimilation impacts spermidine production and other processes.
- Microbial interactions drive metabolic lag phase optimizations.

Keywords

Lag phase, starvation, heterotrophic bacteria, dimethylsulfoniopropionate, one-carbon metabolism, methionine, spermidine, *Emiliania huxleyi*, microbial interactions, osmoprotectants.

Introduction

Marine heterotrophic bacteria rely on organic carbon synthesized by photosynthetic microorganisms, and consume approximately half of the carbon fixed by these primary producers[1–3]. The primary producers, namely microalgae, produce organic carbon by fixing CO_2 in a process that is subjected to temporal dynamics[4,5]. For example, photosynthetic productivity is poor at night and in winter, when light intensities decline or nutrients are depleted. Consequently, heterotrophic bacteria must endure prolonged phases of starvation[6–11]. However, with the onset of microalgal productivity, bacteria must rapidly activate their metabolism. A rapid metabolic response is key for bacteria to outgrow co-occurring competitors[12–14]. The ability of bacteria to rapidly respond to newly produced carbon is

essential for survival and success at sea.

The transition from starvation[15,16] and preparation for cell division occur during the lag phase[17]. Recent studies highlight that bacteria undergo a global metabolic reorganization during the lag phase [18] and synthesize essential building blocks (such as nucleotides and amino acids), which are then incorporated into larger macromolecules including DNA, RNA and proteins[19–23]. Externally added building blocks alleviate metabolic needs during the bacterial lag phase[23]. Since building blocks are exchanged within microbial communities, they are an important currency that drives microbial interactions[24–26]. While the lag phase has been well-studied in human pathogens and in food-spoiling bacteria[18], much is unknown about the bacterial lag phase and its controls in the marine environment.

Several groups of marine heterotrophic bacteria, such as the Roseobacter group[27], evolved strategies to efficiently consume metabolites that are secreted by microalgae. Roseobacters are widely distributed in marine surface waters[28,29] and often found in association with microalgae[1], suggesting that these bacteria have adapted to rapidly utilize microalgal metabolites after phases of starvation. In this study, we sought to understand the post-starvation response of a model Roseobacter species, *Phaeobacter inhibens*, to microalgal metabolites and to determine the underlying mechanisms. Therefore, we analyzed the metabolism of *P. inhibens* while it interacts with microalgae or is supplemented with selected microalgal metabolites. The metabolism of *P. inhibens* and its interaction with microalgae have been previously studied, providing a solid foundation for our current research[30–47].

We discovered that nano- to micromolar concentrations of methylated compounds, which are abundantly produced by microalgae[48–51], significantly shorten the lag phase of bacteria. Specifically, compounds that can donate one-carbon groups to the bacterial metabolism—mainly *N*- and *S*-methylated compounds—were effective, while non-methylated compounds were not effective. In addition, we found that bacterial genes involved in methyl group metabolism were among the 20 highest transcribed metabolic genes during co-cultivation with algae. To elucidate the underlying mechanisms of lag phase shortening by methylated compounds, we explored the bacterial transcriptome during the lag phase, analyzed the incorporation of ^{13}C-labeled methyl groups, estimated cellular methyl group requirements, characterized the role and substrate spectrum of methyl group assimilation enzymes, and screened for lag phase shortening in various bacteria. Our results show that methyl group synthesis is a bottleneck during the bacterial lag phase, and that various bacteria—including *Bacillus subtilis* and *Escherichia coli* strains—achieve shorter lag times when supplemented with methylated compounds. We conclude that bacteria can overcome the bottleneck of methyl group synthesis by assimilating methyl groups from external sources.

The production and secretion of methylated compounds is a hallmark of photosynthetic organisms[48,52,53]. Therefore, it is possible that the ability of bacteria to utilize methyl groups is an adaptation that arose during co-evolution with microalgae. Our findings unveil a fundamental mechanism in the regulation of the bacterial lag phase and highlight the significance of exploring bacterial physiology in an ecological context.

Results

Bacterial methyl group metabolism genes are highly transcribed during co-cultivation with algae

We set out to investigate the metabolic response and the underlying genes that are activated in *Phaeobacter inhibens* bacteria during co-cultivation with *Emiliania huxleyi* microalgae (also known as *Gephyrocapsa huxleyi*[54]). This algal-bacterial pair is environmentally relevant and was previously studied by us and by others[32,36,42,45,46,55]. To understand the bacterial response towards microalgae, we analyzed the transcriptome of bacteria in co-cultures with algae. In these co-cultures, bacteria rely entirely on algal-secreted metabolites for growth[36]. As a reference condition, we analyzed bacterial pure cultures that received glucose as a sole carbon source (Figures S1-S3, Tables S1-S2, and Data S1). First, bacterial transcript abundances were quantified in the presence of algae. We focused on metabolic genes based on KEGG metabolic pathways definitions[56] to identify catabolic and anabolic processes that are highly active in the bacteria. We found that genes involved in utilizing methylated compounds were among the 20 highest transcribed bacterial metabolic genes (Figure 1A and Data S1). These genes are involved in harvesting methyl groups from donor compounds (gene 3; cobalamin-dependent methyltransferase), dissimilating methyl groups for ATP generation (gene 29; formate—THF ligase), utilizing methylated assimilation products for biosynthesis (gene 1, 2 and 21; spermidine synthesis) and replenishing the TCA cycle during growth on specific methylated compounds (gene 10; crotonyl-CoA carboxylase; ethylmalonyl-CoA pathway). We then manually identified bacterial genes that are relevant for metabolizing methylated compounds based on functional annotations, transcript levels and literature reports, which resulted in a list of 83 methyl group metabolism genes (Table S3 and Figure S4). The identified methyl group metabolism genes were markedly upregulated in the presence of algae, compared to bacterial pure cultures grown with glucose, as can be seen from the results of a differential gene expression (DE) analysis (Figure 1B and Data S1 for DE results of all genes). To portray the routes by which bacteria utilize methyl groups during interactions with algae, we overlaid the reactions encoded by the methyl group metabolism genes with the DE results (Figure 1C). This schematic overview of bacterial methyl group metabolism, also termed one-carbon metabolism, highlights that bacteria harvest, dissimilate

and assimilate methyl groups during interactions with algae, indicating that methylated compounds are a relevant resource for algal-associated bacteria.

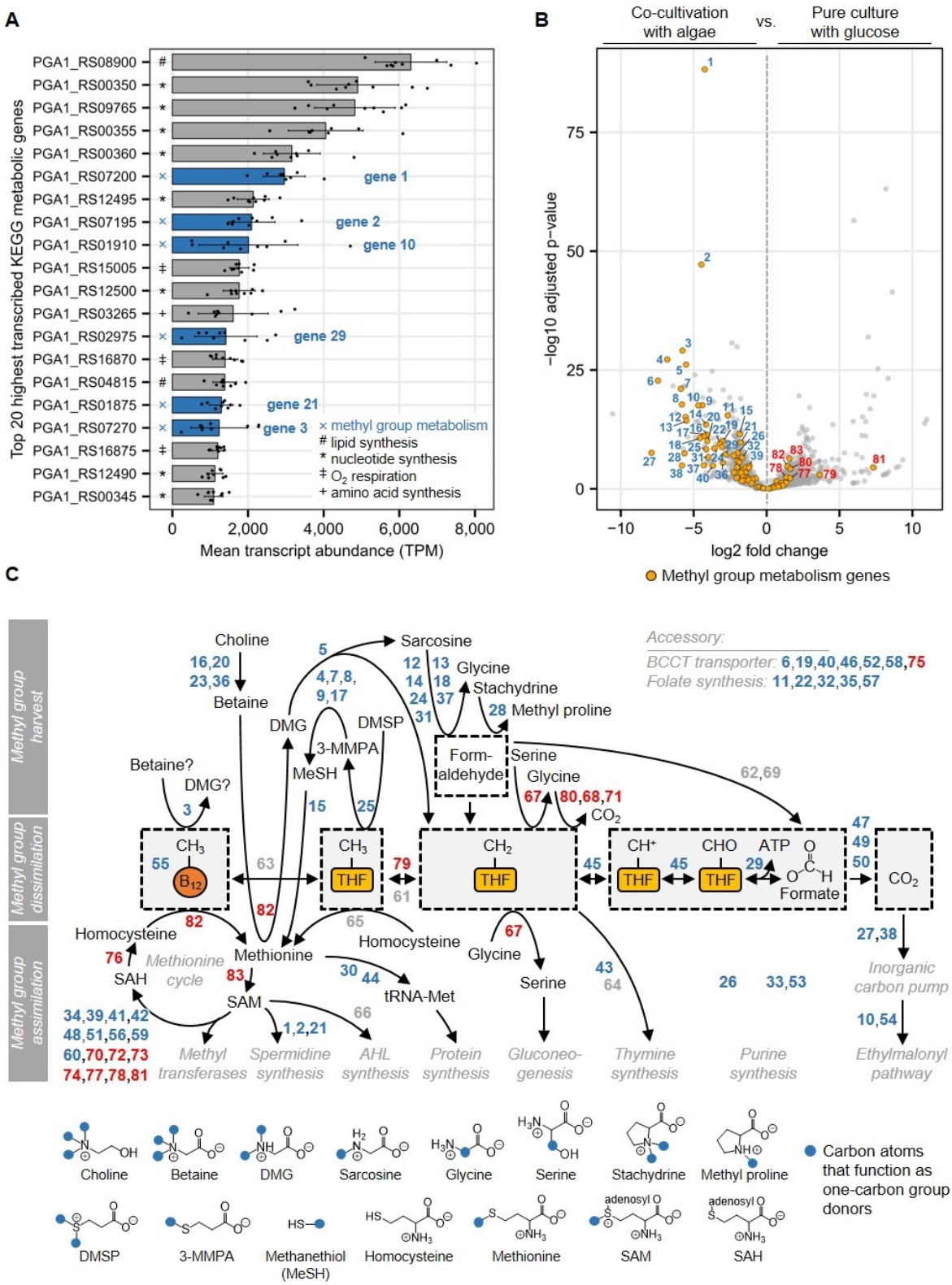

Figure 1: Identification of metabolic genes that are transcribed in *P. inhibens* bacteria during co-cultivation with *E. huxleyi* microalgae. (**A**) Dual RNA-sequencing revealed that bacterial

genes involved in methyl group metabolism were among the highest transcribed KEGG metabolic genes in the presence of algae (blue bars; average of nine co-cultivation samples from day 04 – 09; Figure S1). Labels on the y-axis: RefSeq accession numbers. KEGG annotations of respective methyl group metabolism genes: S-adenosylmethionine decarboxylase (gene 1), trimethylamine—corrinoid protein Co-methyltransferase (gene 3), spermidine synthase (gene 2), crotonyl-CoA carboxylase/reductase (gene 10), formate—tetrahydrofolate ligase (gene 29), ornithine decarboxylase (gene 21). See Data S1 for transcript abundances per sample. (**B**) Methyl group metabolism genes (orange dots) were upregulated in bacteria that were co-cultivated with algae (left; blue numbers) compared to bacteria in pure cultures that grew exponentially with glucose (right; red numbers). (**C**) Bacterial methyl group metabolism genes include reactions involved in harvesting, dissimilating and assimilating methyl groups from methylated donor compounds. Included are genes that are either directly involved in transforming methyl groups, or which are accessory and encode for transporters or tetrahydrofolate (THF) synthesis. Blue and red numbers indicate up- and downregulated genes, respectively (thresholds for coloring: adjusted *p*-value < 0.5; log2 fold change < -0.585 and > +0.585). Gene numbers are identical throughout the text and figures, with accession numbers and functional annotations listed in Table S3. Blue dots in chemical structures represent carbon atoms (mainly methyl groups) that function as one-carbon group donors.

The methylated compound DMSP triggers the shortening of the bacterial lag phase

To investigate the influence of methylated compounds on bacteria, we conducted a series of growth experiments using the *S*-methylated compound dimethylsulfoniopropionate (DMSP) as a model substrate. DMSP is a naturally occurring metabolite that is produced by microalgae and metabolized by various bacteria[53,57–60]. In our experiments, bacterial pure cultures were grown with glucose as a sole carbon source, and supplemented with DMSP. We found that micromolar concentrations of DMSP stimulated the growth of bacteria, compared to bacteria that received only glucose (Figure 2A). By plotting the growth curves on a semi-logarithmic scale, it can be seen that lag times were shortened, while growth rates were not affected (Figure 2B). We further quantified the lag phase shortening effect by calculating △lag times, which is the time difference between the onset of growth in control cultures, compared to supplemented cultures (Figures 2B and S5A). By analyzing △lag times under different DMSP concentrations, we found that lag times were shortened by up to 2.5 hours, and that already nanomolar concentrations of DMSP were effective (Figure 2C, S5B and S5C). Nanomolar concentrations of DMSP are ecologically relevant, as they occur in microalgal-enriched seawater[61]. Overall, our results show that exposure to the methylated compound DMSP leads to the shortening of the bacterial lag phase.

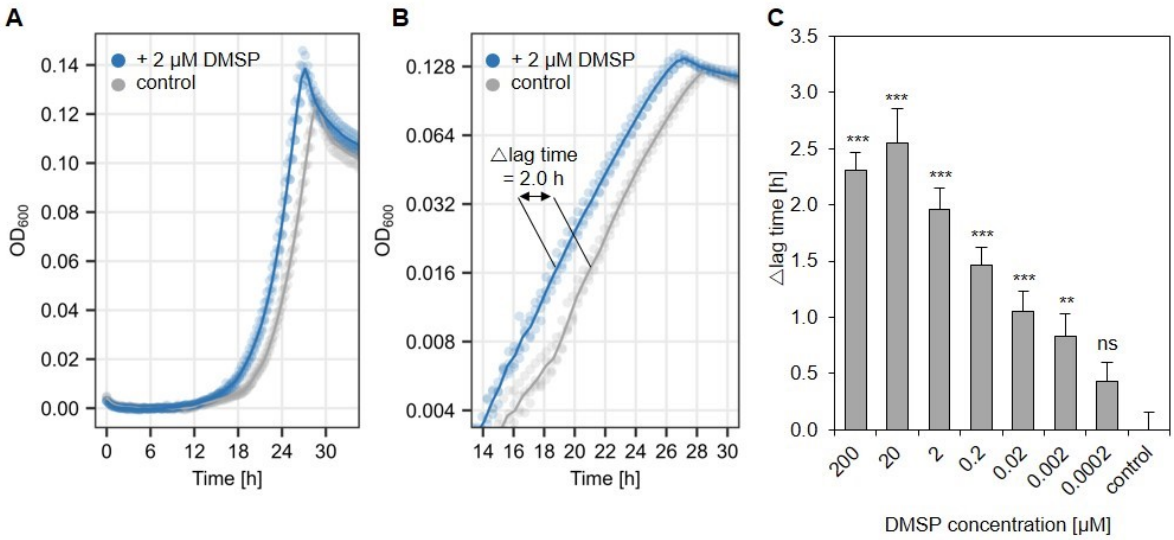

Figure 2: The methylated compound DMSP induces lag phase shortening in *P. inhibens* bacteria. (**A**) Micromolar concentrations of DMSP stimulated earlier growth of bacteria (blue) compared to non-supplemented control cultures (grey). (**B**) Semi-log2 transformed growth curves show that doubling times were unchanged, as evident from the identical slopes, while lag times were shortened. Lag phase shortening is expressed as the mean differences between lag times measured for supplemented cultures compared to control cultures (△lag time; see *Method details* for explanations). (**C**) Exposure to nanomolar concentrations of DMSP resulted in bacterial lag phase shortening. All growth experiments were conducted with four biological replicates in artificial seawater medium (ASW_b) with 1 mM glucose as carbon source. In panels **A** and **B**, dots represent measurements of individual cultures and lines depict a smoothed average of the replicates. Error bars in panel **C** indicate the standard error of the difference between means. ANOVA and Dunnett's test were used to identify significant differences between control and supplemented cultures (adjusted *p*-value thresholds: *** ≤ 0.001, ** ≤ 0.01, ns [not significant] > 0.05).

Methyl groups induce lag phase shortening

To determine whether the methyl groups of DMSP are involved in lag phase shortening, we measured △lag times for analogues of DMSP that harbor different numbers of methyl groups (Figure 3A, S6 and S7). We found that the extent of lag phase shortening correlated with the number of methyl groups per molecule, while non-methylated analogues were ineffective (Figure 3A). This finding suggests that the methyl groups of DMSP are involved in lag phase shortening.

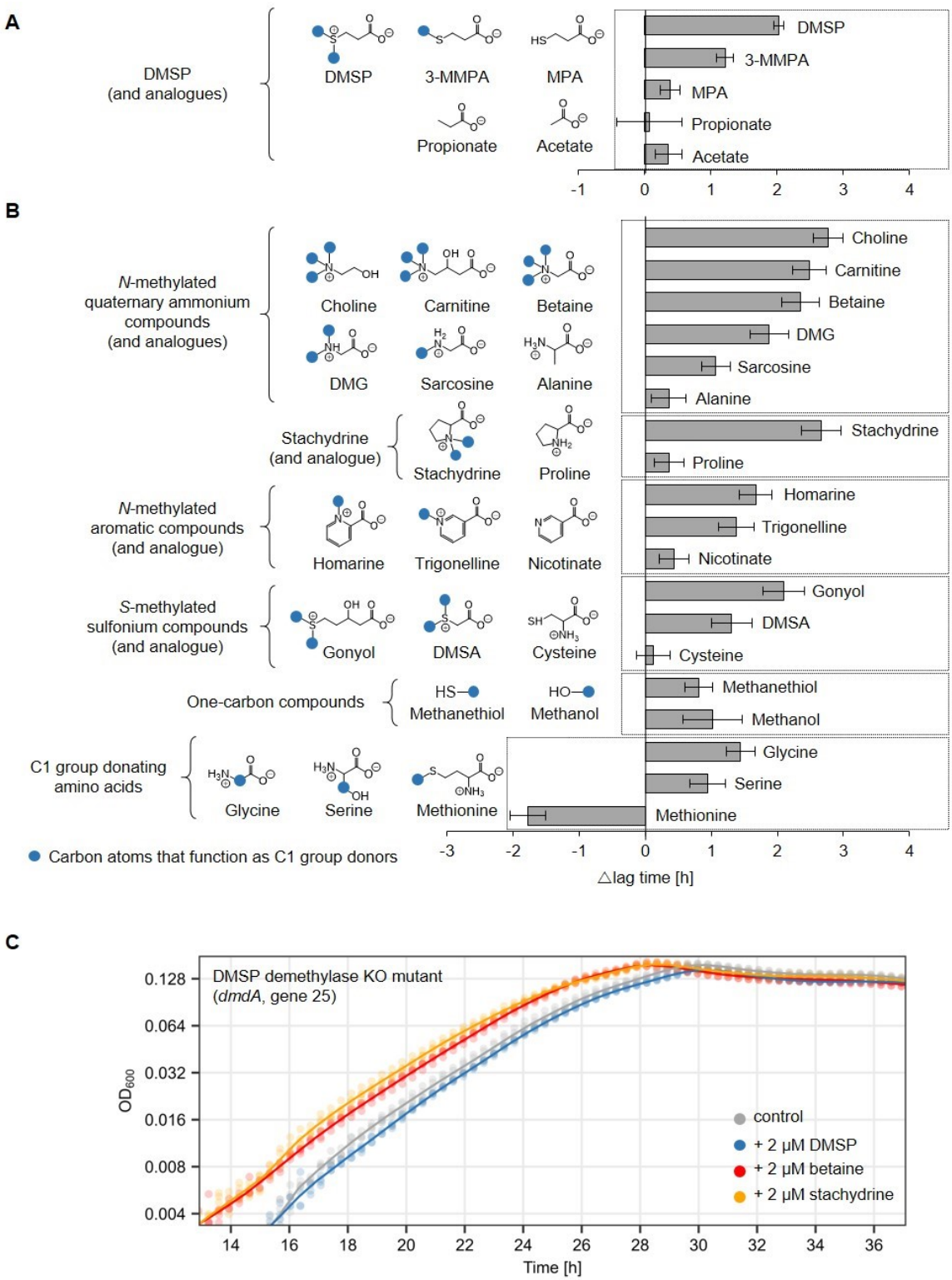

Figure 3: Methyl groups and other one-carbon moieties induce lag phase shortening in *P. inhibens* bacteria. (**A**) Growth experiments with analogues of DMSP revealed that methyl groups are required for lag phase shortening. The number of methyl groups per molecule correlated with the extent of lag phase shortening. (**B**) Growth experiments further revealed that multiple methylated compounds trigger lag phase shortening, while non-methylated analogues were not effective. In panels **A** and **B**, blue dots in chemical structures represent carbon atoms (mainly methyl groups) that function as one-carbon group donors. (**C**) Lag phase

shortening was no longer evident in a *P. inhibens dmdA* knock-out mutant upon exposure to DMSP, while other methylated compounds (betaine and stachydrine) still triggered lag phase shortening. Dots represent measurements of individual cultures and lines depict a smoothed average of four biological replicates.

To investigate whether other methylated compounds induce lag phase shortening, we tested molecules that are commonly produced by microalgae (Figure 3B). We selected methylated compounds with different chemical properties including *N*-methylated, *S*-methylated, small one-carbon compounds and amino acids (which are themselves not methylated but can donate one-carbon groups to the cellular methyl group metabolism). The results show that supplementation with all tested methylated compounds resulted in shortening of the lag phase (Figure 3B), while the doubling times were largely unchanged (Figure S6 and S7). The lag phase shortening effect was most pronounced for *N*-methylated compounds with three or two methyl groups (i.e., carnitine, choline, betaine, stachydrine), and *S*-methylated compounds with two methyl groups (i.e., gonyol and DMSA; Figure 3B). The extent of lag phase shortening correlated with the number of methyl groups per molecule, in line with our results for the DMSP analogues (Figure 3A). Interestingly, methionine was an exception and prolonged the lag phase. Growth inhibitions by methionine were reported for other bacteria and may result from feedback loops that regulate intracellular methionine concentrations[62]. In summary, our results revealed that a wide array of methylated compounds induce the shortening of the bacterial lag phase, while non-methylated analogues do not impact the lag phase.

Demethylase genes are required for lag phase shortening

The involvement of methyl groups in lag phase shortening could be explained by three possible scenarios: 1) methyl groups are a limiting resource, 2) methylated compounds are sensed by receptor proteins that trigger a signal cascade, and 3) methylated compounds act as intracellular solutes with protective functions. To test whether methyl groups are a limiting resource, we generated a *P. inhibens* knock-out (KO) mutant that is unable to harvest methyl groups from a respective donor compound. We deleted the *dmdA* gene (Figure 1C; gene 25), which encodes for the well-characterized DMSP demethylase[57,63,64]. The deletion of the demethylase gene is expected to hamper the harvest of methyl groups from DMSP, while it is not expected to affect extracellular receptor binding or internalization of the compound. Our data show that DMSP-dependent lag phase shortening was abolished in the *dmdA* KO mutant (Figure 3C). Importantly, the mutant still demonstrated lag phase shortening when supplemented with the methylated compounds betaine and stachydrine (Figure 3C). These results suggest that methyl groups are a limiting resource during the lag phase and that

bacteria can overcome this bottleneck by harvesting methyl groups from external donor compounds.

Stoichiometric calculations highlight assimilatory methyl group requirements

Methyl groups may function as a limiting resource either by being assimilated as a one-carbon group (C1) substrate, or by being dissimilated for ATP generation (Figure 1C). To explore the possible fate of methyl groups during the lag phase, we estimated the C1 group requirements per bacterial cell needed for one cell duplication. In this process, C1 groups are utilized as a substrate to synthesize cellular building blocks for biomass formation (i.e., purines, thymine, methionine and histidine; Table S4). Based on numbers determined for exponentially growing *E. coli*[65], we calculated that a single *P. inhibens* cell requires 190.1 amol of C1 groups to synthesize the building blocks needed for one cell duplication (Table S4). If a freshly initiated *P. inhibens* culture (25,000 CFU/mL) assimilates all available DMSP methyl groups during the lag phase, then the bacterial population requires 2.4 nM of DMSP to duplicate. Indeed, similar DMSP concentrations—2 nM—induced significant lag phase shortening (Figure 2C).

Methyl groups could also be dissimilated for ATP generation; a process that yields one ATP per methyl group (Figure 1C; gene 29). The bacterium *E. coli* has an estimated growth and non-growth maintenance cost of 19,096 amol ATP per cell during exponential growth with glucose[66]. Assuming similar ATP costs for *P. inhibens* and that a freshly initiated *P. inhibens* culture (25,000 CFU/mL) dissimilates all available DMSP methyl groups during the lag phase, then the bacterial population requires 238 nM of DMSP to cover 100% of its ATP costs for one duplication. Of note, concentrations of 2 nM DMSP already induced significant lag phase shortening (Figure 2C). This concentration of DMSP methyl groups can cover only 0.8% of the bacterial ATP needs. Based on these calculations, it appears more plausible that DMSP methyl groups are assimilated during the lag phase to cover C1 group requirements, while the required ATP is generated from the glucose in the medium.

Methyl group assimilation genes are upregulated during the lag phase

To experimentally elucidate the intracellular fate of methyl groups, we analyzed the bacterial transcriptome in response to DMSP during the lag phase. Therefore, glucose-grown stationary phase bacteria were used to initiate fresh cultures that contained either glucose as sole carbon source, or which were supplemented with DMSP. RNA was sampled 15 min and 40 min after initiation of the cultures (Figures S8-S10, Tables S5-S6, and Data S2). Our data show that the addition of DMSP resulted in the upregulation of methyl group metabolism genes during the lag phase (Figures S1-S13)—an effect that was most pronounced 15 min post initiation of

fresh cultures. Specifically, genes involved in DMSP catabolism were upregulated (Figure S11; genes 4, 7, 8, 9, 17, 25), including the DMSP demethylase gene (*dmdA*: gene 25). The most upregulated genes were involved in synthesizing spermidine (Figure S11; genes 1, 2 and 21), which is a metabolite that is associated with cell growth[67]. The most downregulated gene was involved in methyl group oxidation—a regulation that may impede methyl group dissimilation (Figure S11; gene 79). Interestingly, DMSP demethylation (*dmdA*: gene 25), spermidine synthesis (*speD*: gene 1, *speE*: gene 2, and gene 21) and methyl group oxidation (*metF*: gene 79) are all linked via the methionine cycle (Figure 4A). This link is further supported by the upregulation of *metK* (gene 83)—a gene that is involved in converting methionine into *S*-adenosylmethionine (SAM; Figure 4A). Of note, it was previously reported that methionine synthesis in *P. inhibens* depends on a split methionine synthase, which is encoded by three genes[68]. However, the three genes were not transcriptionally co-regulated in our transcriptomics experiment (Figure 4A; genes 55, 63, and *bmt*: gene 82)—an observation that is further addressed below. In summary, transcriptome analyses suggest that DMSP methyl groups are assimilated during the bacterial lag phase through the methionine cycle.

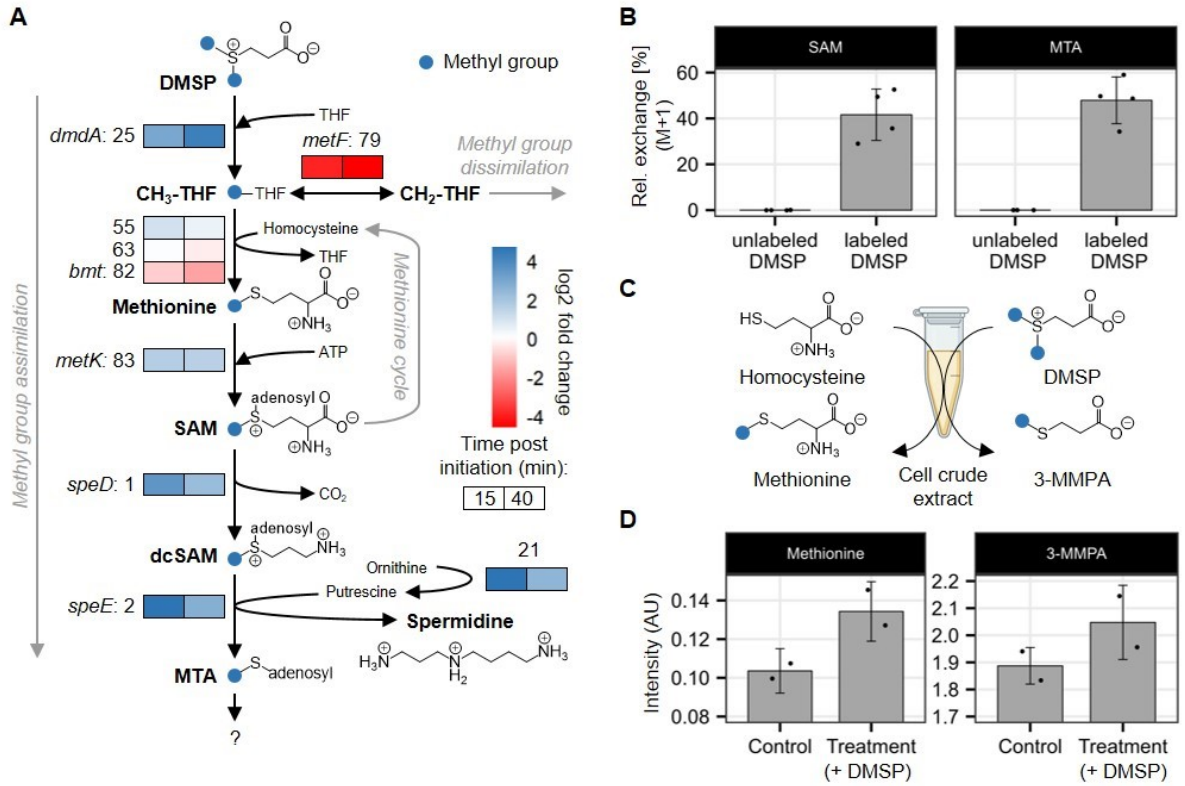

Figure 4: Transcriptional, metabolic and enzymatic response of *P. inhibens* bacteria towards DMSP. (**A**) The transcriptional response was analyzed in freshly initiated bacterial cultures that were supplemented with 50 µM DMSP, compared to control cultures without DMSP (all cultures contained 1 mM glucose). Gene expression changes (log2 fold change) are indicated

as colored boxes that correspond to the age of the culture post initiation—15 min (left box) and 40 min (right box). Colors show upregulation (blue) and downregulation (red) in response to DMSP. The three most upregulated methyl group metabolism genes were involved in spermidine synthesis (*speD*, *speE* and gene 21; Figure S11). Spermidine synthesis utilizes *S*-adenosylmethionine (SAM), which is the main product of the methionine cycle. Likewise, genes involved in DMSP demethylation (*dmdA*) and SAM synthesis (*metK*) were highly upregulated in response to DMSP. A gene that mediates between methyl group assimilation and dissimilation was the most downregulated gene in response to DMSP (*metF*; Figure S11). Numbers left to boxes or above designate gene numbers (see Table S3 for accession numbers and functional annotations). (**B**) Tracking the metabolic fate of DMSP methyl groups during the lag phase. Freshly initiated bacterial cultures were supplemented with 50 µM [^{13}C-methyl]DMSP, in which both methyl groups are ^{13}C-labeled. The intracellular formation of ^{13}C-labeled metabolites was monitored 2 hours after initiation by LC-MS analysis. The method identified ^{13}C-labeled SAM (rel. exchange for M+1: 41.6%) and ^{13}C-labeled 5'-methylthioadenosine (MTA; rel. exchange for M+1: 47.9%). (**C**) Evaluating methionine synthesis activity in response to DMSP. Cell crude extracts were generated from stationary phase bacteria that were treated for 2 hours with 1 µM DMSP. The cell crude extracts were then used for *in vitro* reactions with added homocysteine and DMSP to catalyze the enzymatic formation of methionine and 3-*S*-methylmercaptopropionate (3-MMPA), which is the demethylated form of DMSP. Product formation was measured by LC-MS analysis. (**D**) Cell crude extracts from DMSP-treated bacteria produced more methionine and 3-MMPA, compared to cell crude extracts from untreated control cultures.

^{13}C-labeled DMSP methyl groups are assimilated during the lag phase

To further elucidate the cellular fate of methyl groups, we wished to identify metabolites that are synthesized from the methyl groups of DMSP during the lag phase. Therefore, bacteria were supplemented with [^{13}C-methyl]DMSP in which both methyl group carbons were labeled. In this experiment, glucose-grown stationary phase bacteria were used to initiate fresh cultures that contained glucose as a sole carbon source, and to which either [^{13}C-methyl]DMSP or unlabeled DMSP were added. Cells were harvested two hours after initiation of fresh cultures (Figure S8) and then subjected to metabolite extraction and LC-MS analysis. Our results show that DMSP methyl groups were incorporated into SAM and *S*-methyl-5'-thioadenosine (MTA) with relative exchange values of 41.6% and 47.9%, respectively (values given for M+1 isotopologues with single ^{13}C label; Figure 4B). SAM is formed via the methionine cycle and is required, among others, as a substrate for spermidine synthesis. MTA is a methylated side product of spermidine synthesis (Figure 4A). The formation of ^{13}C-labeled SAM and MTA confirms that DMSP-derived methyl groups are assimilated via the methionine cycle. The exchange rates were similar for both compounds, indicating that the majority of produced SAM is converted to MTA. We cannot exclude that DMSP methyl groups are also used for other processes, such as purine synthesis (Figure S12), however, results of [^{13}C-methyl]DMSP LC-MS analysis are in accordance with the transcriptional upregulation of spermidine synthesis genes in response to DMSP (Figure 4A). These results demonstrate that DMSP methyl groups are assimilated during the bacterial lag phase through the methionine cycle.

DMSP stimulates enzymatic methionine synthesis

Next, we investigated whether DMSP activates enzymes that are involved in utilizing DMSP methyl groups for methionine synthesis. Based on previous reports, DMSP-dependent methionine synthesis in *P. inhibens* begins with the transfer of a methyl group from DMSP to tetrahydrofolate (THF) by a demethylase encoded by *dmdA*[69]. Then, methylated THF (methyl-THF) is used for methionine synthesis[33,68]. The methionine synthase of *P. inhibens* is encoded by three genes, which are involved in binding a cobalamin co-factor (vitamin B_{12}; gene 55), transferring the methyl group of methyl-THF to cobalamin (gene 63), and utilizing methylated cobalamin for the methylation of homocysteine (*bmt*), which results in methionine[68]. Our RNA-sequencing data and [^{13}C-methyl]DMSP LC-MS results showed that DMSP methyl groups are assimilated through the methionine cycle, however, the transcription levels of the three bacterial split methionine synthase genes were variable (Figure 4A; gene 55, 63 and *bmt*). In fact, the key gene for methionine synthesis (*bmt*: gene 82) was downregulated in response to DMSP (Figure 4A). While *bmt* downregulation appears contradictory at a first look, it is in line with previous reports that showed feedback regulation of bacterial methionine cycle components in response to their own products[62,70]. The downregulation of *bmt* could thus prevent the accumulation of inhibitory methionine, which we found was the only compound that extended the lag phase of *P. inhibens* (Figure 3B). To clarify the effect of DMSP on methionine formation, we measured methionine synthesis activity in DMSP-treated cells and control cultures. For this assay, cell crude extracts were generated from stationary phase bacteria that were treated for 2 hours with DMSP. The resulting crude extracts, which contained all cellular components, including THF and cobalamin, were then incubated with the substrates for methionine synthesis—homocysteine and DMSP. Enzymatic formation of the products methionine and 3-MMPA (the demethylated form of DMSP) was measured by LC-MS analysis (Figure 4C). Our data show that crude extracts of DMSP-treated cells produced more methionine and 3-MMPA (Figure 4D), indicating that methionine synthesis was increased in those samples. In conclusion, despite the transcriptional downregulation of *bmt*, the methionine cycle appears to be activated in DMSP-treated bacteria.

Bmt is a methionine synthase that utilizes DMSP as a methyl group donor

To further investigate the mechanism by which DMSP methyl groups are utilized for methionine synthesis, we aimed to characterize the underlying enzymatic machinery. As previously outlined, the reported route for DMSP-dependent methionine synthesis in *P. inhibens* proceeds via the sequential transfer of a methyl group from DMSP to THF (*dmdA*: gene 25), to cobalamin (gene 55 and 63) and finally to homocysteine (*bmt*: gene 28), resulting in methionine (Figure 1C). However, an alternative route may exist. It was shown that

homologues of the enzyme Bmt (encoded by the *bmt* gene) can directly transfer methyl groups from a variety of methylated compounds directly to homocysteine, without involving THF or cobalamin as methyl group carriers. For example, the Bmt homologue in human, named BHMT, directly uses a methyl group from *N*-methylated betaine or *S*-methylated DMSA for methionine synthesis[71,72]. A similar substrate spectrum was reported for the Bmt of the bacterium *Sinorhizobium meliloti*[73]. The Bmt homologue in *E.coli* (MmuM[74,75]) and the BHMT-2 enzyme in human[76] can both transfer a methyl group directly from *S*-methylated *S*-methylmethionine (SMM). Furthermore, it was reported that mammalian Bmt homologues utilize DMSP as a methyl group donor[77,78]. These previous reports raised the possibility for direct DMSP demethylation coupled to methionine synthesis by Bmt, without involving DmdA or other split methionine synthase components—a metabolic route that was not yet reported in marine bacteria.

To determine whether the Bmt of *P. inhibens* transfers methyl groups from DMSP directly to homocysteine, we conducted an *in vitro* assay with purified enzyme. Bmt was expressed in a heterologous system and purified by affinity chromatography (Figure S14). The purified Bmt enzyme was then incubated with either DMSP or betaine as methyl group donors, and homocysteine as a methyl group acceptor. Purified *E. coli* MmuM was used as a positive control with SMM as a methyl group donor[74]. A commercial fluorescence-based kit was used to measure methionine formation. Our results show that Bmt indeed produced methionine *in vitro* by transferring a methyl group directly from DMSP to homocysteine (Figure 5). The Bmt enzyme of *P. inhibens* also utilized betaine as a methyl group donor (Figure 5). Our results do not exclude the possibility that Bmt is part of a split methionine synthase *in vivo*[68], however, the results highlight that the Bmt enzyme could be an alternative route for DMSP demethylation in marine bacteria. These findings may also explain why the three split methionine synthase genes were not transcriptionally co-regulated in response to DMSP (Figure 4A; gene 55, 63 and *bmt*: gene 82). Of note, Bmt cannot substitute DmdA *in vivo*, since DMSP-dependent lag phase shortening was abolished in the *dmdA* knock-out mutant, despite the presence of a *bmt* gene (Figure 3C). Taken together, our data demonstrate that the *P. inhibens* Bmt can act *in vitro* as a methionine synthase, using different methylated compounds as methyl group donors. These findings suggest metabolic flexibility in the harvesting and assimilation of various methyl groups from methylated compounds in the environment.

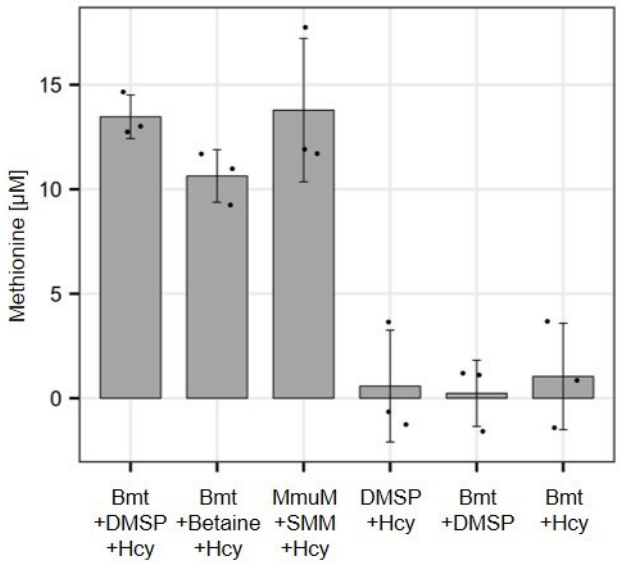

Figure 5: The *P. inhibens* methionine synthase Bmt utilizes DMSP and betaine as methyl group donors. The formation of methionine was quantified using *in vitro* reactions containing purified Bmt together with the methyl group acceptor homocysteine (Hcy) and the methyl group donors DMSP or betaine. The purified methionine synthase MmuM from *E. coli* was used as a positive control, which utilizes *S*-methyl-L-methionine (SMM) as the methyl group donor. Results were compared to negative control reactions in which a single component was omitted (either Bmt, Hcy or DMSP). Dots represent the results of three independent experiments and error bars indicate the standard deviation.

Bmt is required for lag phase shortening

To evaluate whether Bmt plays a role in lag phase shortening *in vivo*, we deleted the *bmt* gene in *P. inhibens.* The *bmt* KO mutant showed impaired growth in the absence of methionine, which was restored upon adding methionine (Figure 6A). Under both conditions, with and without methionine, DMSP did not induce shorter lag times in the *bmt* KO mutant (Figure 6A). This suggests that the Bmt methionine synthase is involved in lag phase shortening, and is required together with DmdA for a lag shortening response towards DMSP.

Of note, residual growth was observed in the *bmt* KO mutant in the absence of methionine (Figure 6A). This growth might result from the presence of a second methionine synthase, namely MetE[79]. The MetE enzyme, which uses methyltetrahydrofolate as a methyl group donor for cobalamin-independent methionine synthesis (Figure 1C; gene 65), could partially compensate for the missing Bmt[80]. However, the *metE* gene was poorly expressed under all tested conditions (Figures S4 and S13; gene 65). To evaluate whether MetE is involved in lag phase shortening, we generated a corresponding KO mutant. The *metE* KO mutant exhibited lag phase shortening upon supplementation with DMSP (Figure 6B). Thus, the methionine synthase Bmt, but not MetE, is involved in lag phase shortening in *P. inhibens* bacteria.

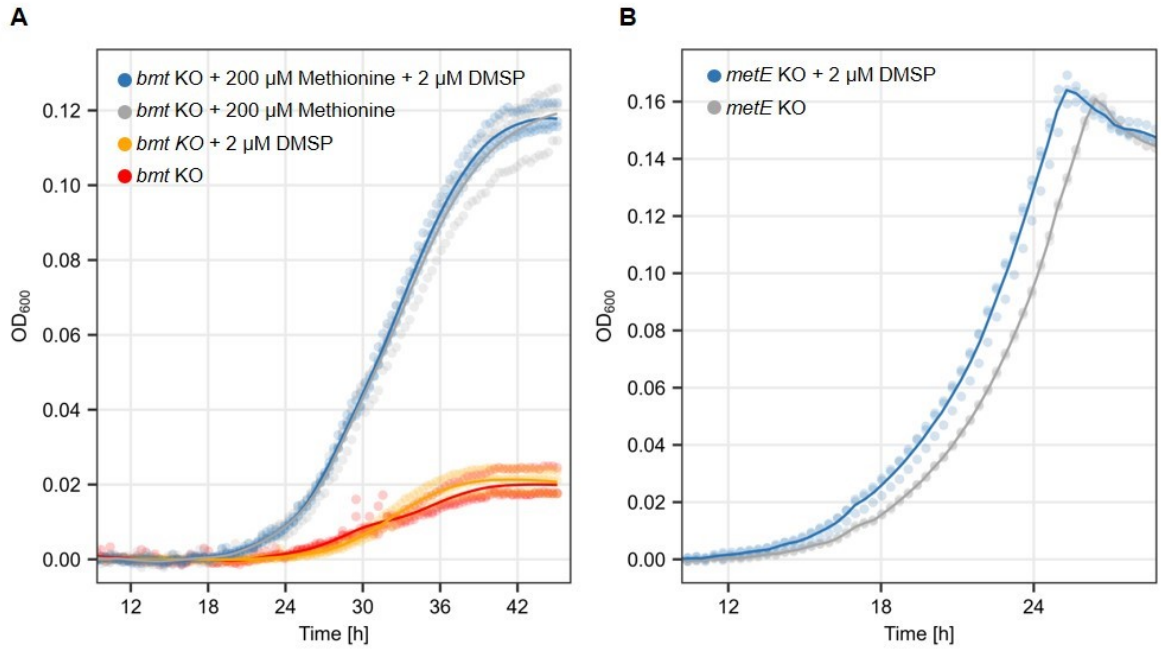

Figure 6: The *P. inhibens* methionine synthase gene *bmt* is required for lag phase shortening. **(A)** Growth of the *bmt* KO mutant was impaired in the absence of methionine (red) but was restored upon adding 200 µM methionine to the medium (grey). The supplementation of bacteria with 2 µM DMSP did not affect the lag time of the *bmt* KO mutant, neither in the presence of methionine (orange), nor in its absence (blue). **(B)** The *P. inhibens* methionine synthase *metE*, which encodes for an enzyme that utilizes methyltetrahydrofolate as methyl group donor, is not involved in lag phase shortening. The *metE* KO mutant still exhibited lag phase shortening upon supplementation with 2 µM DMSP (blue), compared to control cultures (grey). Dots represent measurements for individual cultures and lines depict a smoothed average of three biological replicates.

Methylated compounds shorten the lag phase in various bacteria

To determine whether lag phase shortening occurs in other bacteria, we tested the effect of methylated compounds in bacteria with different lifestyles. A variety of marine bacteria showed lag phase shortening in response to small amounts of DMSP or betaine (Figures 7A, S15A and S15B). Since methylated compounds are often produced by photosynthesizing organisms, we also tested plant-associated bacteria. Our results showed that these bacteria exhibited considerable lag phase shortening in response to betaine, and to a lesser extent to DMSP (Figures S15C and S15D). Notably, the model plant-associated bacterium *B. subtilis* exhibited a △lag time of 10 hours upon treatment with betaine (Figure 7B). The opportunistic pathogens *Pantoea agglomerans* and *Ewingella americana*, which are found both in plants and humans[81,82], also showed shorter lag phases in response to *S*-methyl-L-methionine (SMM, Figure S15C and S15D)—a methylated compound that is highly abundant in plants[83]. Finally, we tested the model bacterium *E. coli*, which occurs in the gut and is, therefore,

unlikely to respond to algal metabolites. Indeed, treatment with either DMSP or betaine did not shorten the lag phase of *E. coli*. However, treatment of *E. coli* with the methyl group donor SMM resulted in a △lag time of one hour (Figure 7C). This effect was observed in *E. coli* strains BL21(DE3) and DH5α, while the wild-type strain K12 required higher concentrations of SMM (Figures 7C, S15E and S15F). Our data show that lag phase shortening induced by methylated compounds occurs in bacteria with different lifestyles. The response of the bacteria to specific compounds may reflect the natural environments in which these bacteria have evolved.

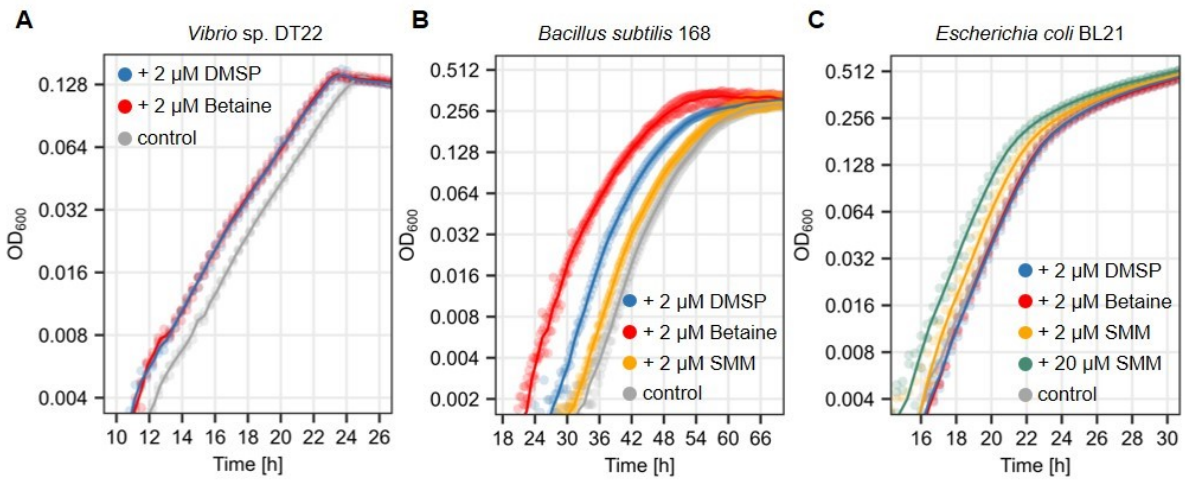

Figure 7. Methylated compounds induce lag phase shortening in diverse bacteria. Lag phase shortening was observed in (**A**) the marine bacterium *Vibrio* sp. DT22 supplemented with DMSP and betaine, (**B**) the plant-associated bacterium *Bacillus subtilis* 168 supplemented with DMSP and betaine (C) and the gut bacterium *E. coli* BL21 supplemented with *S*-methyl-L-methionine (SMM). Dots represent measurements for individual cultures and lines depict a smoothed average of three biological replicates.

Discussion

Methylated compounds as C1 group donors versus protective solutes

Our data show that methyl group synthesis during the lag phase of bacteria is a bottleneck that can be alleviated by the external addition of methyl group donors. Our study was motivated by the observation that *N*- and *S*-methylated compounds shorten the lag phase of *P. inhibens* bacteria, while non-methylated analogues were not effective (Figure 3). The positive effect of methylated compounds on bacterial growth was previously reported for other bacteria, but discussed in a different context[84–90]. Specifically, beneficial growth effects were attributed to the role of methylated compounds as osmoprotectants, antioxidants or

thermoprotectants under various stresses. While it is widely acknowledged that cells accumulate methylated compounds as protective solutes[91], our findings do not support a link between solute accumulation and lag phase shortening in *P. inhibens*. As an example, proline is a well-studied protective solute[92–94]. However, our data show that only the methylated form of proline (stachydrine) shortened the lag phase, while proline itself was not effective (Figure 3B). Similarly, lag phase shortening correlated with the number of methyl groups present on DMSP and its analogues (Figure 3A). In addition, the deletion of the DMSP demethylase gene *dmdA* abolished lag phase shortening in DMSP-supplemented bacteria, highlighting the centrality of the methyl groups in triggering lag phase shortening. Finally, ^{13}C-labeled methyl groups of [^{13}C-methyl]DMSP were incorporated into biosynthetic products shortly after initiation of fresh cultures. This confirmed that DMSP methyl groups are assimilated, strengthening the link between methyl group harvest, assimilation and lag phase shortening. Our results thus offer an additional explanation for the beneficial effects of methylated compounds in stressed bacteria; while growth stimulations may arise from solute accumulation, the assimilation of methyl groups can further contribute to the effects. The latter is supported by previous observations that methyl groups are rapidly assimilated in bacterial cultures and natural environments[59,95–101].

Methyl groups are a resource that regulates growth

Imbalances in methyl group metabolism, also termed C1 metabolism, are associated with human diseases[102] and bacterial growth perturbations[103]. The major role of methyl group metabolism is to provide C1 groups for the synthesis of building blocks such as purines (adenine and guanine), thymine, methionine and histidine[103,104]. Additional methyl groups are required to methylate DNA, RNA and proteins[105–107]. It was previously shown that the depletion of building blocks results in longer lag phases[23], and that the synthesis of building blocks is upregulated during the lag phase of bacteria[19–22]. Deficiencies in macromolecule methylations can impair growth by influencing the cell cycle[108], the circadian clock[109] and chemotaxis proteins[110]. It is, therefore, plausible that an insufficient availability of C1 groups during the lag phase will delay building block synthesis and macromolecule methylations. Bacteria generate C1 groups from glucose via the formation of serine and glycine (involving the serine hydroxymethyltransferase and/or a glycine cleavage system[104,111]); however, external methyl group donors could represent a beneficial shortcut (Figure 1C). Indeed, it was shown that glucose-grown Roseobacter bacteria build the majority of their methionine from the methyl groups of supplemented DMSP[95]. Moreover, we found that methyl groups can be directly assimilated from DMSP for the synthesis of methionine—a reaction that is catalyzed by a single enzyme, namely Bmt (Figure 5), and which represents an additional shortcut to the

described routes of methionine synthesis[68,95]. Whether methyl groups are exclusively used for biomass formation, or are also used for ATP generation[112,113], remains to be explored. While our stoichiometric calculations indicate that supplemented methyl groups cover only a small fraction of the ATP costs in cultures with significant lag phase shortening (Figure 2C), it is important to note that a gene involved in ATP generation was transcriptionally upregulated in response to DMSP during the lag phase (*fhs*: gene 29; Figures S11 and S12). Another open question is whether methylated compounds suppress the formation of non-growing subpopulations, which can further contribute to the length of the lag phase[114,115].

Lag phase C1 metabolism and translation initiation

The bacterial methyl group metabolism is intertwined with the translation apparatus[103]. Translation initiation, which is considered to be the rate-limiting step in protein synthesis[103], starts with the initiator fMet-tRNA^{fMet} that provides formylated methionine (fMet) as the first amino acid[116]. To synthesize the initiator fMet-tRNA^{fMet}, at least two C1 groups are required, which are incorporated in the precursors methionine and *N*-formylmethionine. Perturbations in fMet-tRNA^{fMet} synthesis were shown to impair bacterial growth[117,118]. Similarly, it was shown that bacteria exhibit longer lag times when they harbor a defect in a gene that charges tRNA^{Met} with methionine (*metG*[119]). In our transcriptome analyses, the same *metG* gene was markedly upregulated in DMSP-supplemented *P. inhibens* bacteria during the lag phase (gene 44; Figure S11). Moreover, we found that various genes involved in adding C1 modifications to tRNA and rRNA components of the translation apparatus were upregulated during the lag phase (e.g., genes 39, 41, 42, 43; Figure S11 and Table S3). Thus, our data indicate a link between methyl group assimilation and translation initiation.

Lag phase-related regulation of the methionine cycle

The methionine cycle is central in the regulation of the bacterial lag phase. Methionine was the only methylated compound that prolonged the lag phase of *P. inhibens* (Figure 1C). This effect can be either attributed to methionine directly, or to the accumulation of methionine cycle products such as homocysteine or SAM. The methionine cycle is tightly feedback-regulated, explaining the absence of methionine overproducing bacteria outside the lab[120]. Similarly, imbalances in methionine synthesis are associated with diseases in higher organisms[121,122]. A negative feedback regulation was described for an *E. coli* enzyme that synthesizes homocysteine (MetA; homoserine *O*-succinyltransferase), showing that the enzyme is inhibited by methionine and SAM[70,123]. It was also demonstrated that methionine and/or homocysteine inhibit the growth of *E. coli* under certain conditions[62,124]. Moreover, the breakdown of methionine synthesis results in longer lag phases in *E. coli*[125]. In line with tight

feedback-regulation of the methionine cycle, our data show that the methionine synthase gene *bmt* was downregulated in DMSP-supplemented bacteria during the lag phase (Figure 4). Similarly, a homologues *bmt* gene was downregulated in a related Roseobacter bacterium when exposed to DMSP (accession: B5M07_08905[126]). We conclude that the methionine cycle controls the length of the lag phase and that an increased influx of methyl groups into the methionine cycle can be balanced by downregulating the transcription of the methionine synthase gene. In support, our experiments with a *bmt* methionine synthase KO mutant showed that this gene is required for lag phase shortening triggered by methylated compounds, possibly by interfering with the regulatory control of the methionine cycle.

Spermidine and the lag phase

Our results show that spermidine plays a key role during the bacterial lag phase. Specifically, the lag phase transcriptomics results showed pronounced upregulation of the *metK* gene in DMSP-supplemented bacteria. This gene is involved in transforming methionine into SAM[127], which is the precursor for spermidine synthesis (Figure 4A). Moreover, the three most upregulated methyl group metabolism genes were associated with the conversion of SAM into spermidine—a pathway that yields MTA as a side product (genes 1, 2 and 21; Figure S11). Likewise, we found that ^{13}C-labeled DMSP methyl groups were incorporated into SAM and MTA during the lag phase (Figure 4B). Spermidine synthesis genes were also among the 20 highest transcribed metabolic genes in bacteria during co-cultivation with algae (genes 1, 2 and 21; Figure 1A), and they were markedly downregulated in bacteria grown with glucose (Figure 1B). Spermidine is a polycationic polyamine that interacts with negatively charged macromolecules, mainly RNA, and has various cellular functions[67,128]. It was previously shown that *E. coli* mutants with deficient polyamine synthesis exhibit 3-fold lower growth rates in the absence of externally added polyamines[129–131]. Polyamines are also known to enhance the survival of bacteria under stress conditions[132–136]. The benefits of polyamines are often linked with protein synthesis[137], and indeed externally supplemented polyamines can increase protein synthesis by up to 2-fold[128]. The transcription of polyamine transporters was shown to be upregulated during the lag phase of *E. coli*[138], and polyamines induced the transcription of key bacterial genes involved in cell growth[67]. Taken together, our data point to the centrality of polyamine synthesis, and specifically spermidine, during the bacterial lag phase.

The bacterial lag phase in an environmental context

The metabolism of algal-associated bacteria is fueled by algal-produced metabolites. Thus, the bacterial diet naturally includes methylated compounds that are a hallmark for photosynthetic organisms[48–53]. Our findings suggest that algal-associated bacteria optimized

their metabolism to efficiently harvest and assimilate methyl groups from algal donor compounds. While bacteria are capable of synthesizing C1 groups from glucose, harvesting methyl groups from host metabolites can provide a metabolic shortcut. In the marine environment, expediting the transition from lag phase to exponential growth could be critical to compete with other marine bacteria for valuable algal resources. The bacterial ability to rapidly initiate growth when nutrients become available is an important step in outgrowing competitors. Maximizing the efficiency of resource utilization when resources are available, presents a selective advantage to bacteria[139]. Our study provides a glimpse into the fundamental yet overlooked physiology of the bacterial transition from starvation to growth, highlighting the gap in our understanding of non-growing bacteria and the mechanisms that allow them to commence growth.

Acknowledgments

We appreciate the technical guidance of Dr. Ester Feldmesser, Dr. Bareket Dassa, Dr. Shifra Ben-Dor and Dr. Hadas Keren-Shaul in RNA-sequencing, are thankful for the help of Dr. Ron Rotkopf with statistical analysis, and acknowledge the contribution of Dr. Maxim Itkin with LC-MS analysis (Life Sciences Core Facilities, Weizmann Institute of Science, Israel). We thank Dr. Roi Avraham and Dr. Gili Rosenberg (Weizmann Institute of Science, Israel) for sharing their expertise in dual RNA-sequencing. The compound gonyol was synthesized and kindly provided by Dr. Kathleen Thume and Prof. Georg Pohnert (Friedrich Schiller University, Jena, Germany). We are grateful for inspiring discussions with Dr. Torsten Schubert and Jonathan Hammer (Friedrich Schiller University, Jena, Germany) about cobalamin-dependent one-carbon metabolism, and highly appreciate the stimulating feedback we received from Dr. Elad Noor (Weizmann Institute of Science, Israel), Prof. Uwe Sauer (ETH Zürich, Switzerland) and Dr. Anat Bren (Weizmann Institute of Science, Israel) about bacterial metabolism and the lag phase. We are specifically thankful for the conceptual guidance and encouragement from the late Prof. Dan Tawfik (Weizmann Institute of Science, Israel) during the early phase of the study. M.S. received a Dean of Faculty Fellowship, a Sir Charles Clore Fellowship (Clore Israel Foundation) and a Senior Postdoc Fellowship. D.A.N.B received the Armando and Maria Jinich Fellowship. The study was funded by the Minerva Foundation with funding from the German Federal Ministry for Education and Research, the Israel Science Foundation (ISF 947/18), the European Research Council (ERC StG 101075514) and the de Botton center for marine sciences, granted to E.S.

Author contributions

M.S., D.A.N.B. and E.S. designed the study. M.S., D.A.N.B., S.M., V.F. and L.Y. performed and analyzed experiments. J.R. contributed to the design of the research and helped supervise the project. M.S., D.A.N.B. and E.S. wrote the manuscript. All authors discussed the results and contributed to the final manuscript.

Declaration of interests

The authors have a pending patent application and other than that declare no competing interests.

STAR Methods

Key Resources Table

REAGENT or RESOURCE	SOURCE	IDENTIFIER
Bacterial and algal strains		
Emiliania huxley CCMP3266	Bigelow National Center for Marine Algae and Microbiota (NCMA)	N/A
Phaeobacter inhibens DSM 17395; wild type	German Collection of Microorganism and Cell Cultures (DSMZ)	N/A
Phaeobacter inhibens DSM 17395; *dmdA::aacC1* (Gm^r) KO mutant	This paper	ES146
Phaeobacter inhibens DSM 17395; *bmt::aacC1* (Gm^r) KO mutant	This paper	ES124
Phaeobacter inhibens DSM 17395; *metE::aph* (Km^r) KO mutant	This paper	ES138
Vibrio sp. DT22	Despotović *et al.*[140]	N/A
Ruegeria sp. DT77	Despotović *et al.*[140].	N/A
Sulfitobacter pontiacus iR4	Beiralas *et al.*, *under review*	N/A
Bacillus subtilis 168	Bacteriology Unit of The Weizmann Institute of Science, Israel	N/A
Escherichia coli strain BL21 DE3 pLysS	Bacteriology Unit of The Weizmann Institute of Science, Israel	N/A
Escherichia coli strain DH5α	Bacteriology Unit of The Weizmann Institute of Science, Israel	N/A

Escherichia coli strain K-12 MG1655	Bacteriology Unit of The Weizmann Institute of Science, Israel	N/A
Pantoea agglomerans Pag2	Friedman lab strain collection[141]	N/A
Ewingella americana EA	Friedman lab strain collection[141]	N/A
Chemicals, peptides, and recombinant proteins		
Yeast extract	Sigma-Aldrich, Merck	Cat#Y1625
Tryptone	Sigma-Aldrich, Merck	Cat#T7293
Sea salts	Sigma-Aldrich, Merck	Cat#S9883
Bacto™ Agar	BD	Cat#214010
L1 Medium Kit - Si (includes f/2 vitamins, L1 trace elements and L1 nutrients solutions)	Bigelow National Center for Marine Algae and Microbiota (NCMA)	Cat#MKL11000L-Si
D-(+)-Glucose	Sigma-Aldrich, Merck	Cat#G7021
Dimethylpropiothetin HCl, ≥ 96.0%, (dimethylsulfoniopropionate, DMSP)	Sigma-Aldrich, Merck	Cat#80828; CAS: 4337-33-1
3-(Methylthio)propionic acid, 98%, (3-*S*-methylmercaptopropionate, 3-MMPA)	Alfa Aesar	Cat#L12861; CAS: 646-01-5
3-Mercaptopropionic acid, 99%, (MPA)	Alfa Aesar	Cat#A13261; CAS: 107-96-0
Sodium propionate, ≥99%	Sigma-Aldrich, Merck	Cat#P1880; CAS: 137-40-6
Sodium acetate, ≥99%	Sigma-Aldrich, Merck	Cat#S5636; CAS: 127-09-3
Choline chloride, ≥98%	Sigma-Aldrich, Merck	Cat#C7527; CAS: 67-48-1
L-Carnitine, ≥98%	Sigma-Aldrich, Merck	Cat#C0158; CAS: 541-15-1
Betaine, ≥99%	Sigma-Aldrich, Merck	Cat#61962; CAS: 107-43-7
N,*N*-Dimethylglycine HCl, 99%	Acros Organics	Cat#204660050; CAS: 2491-06-7
Sarcosine, 98%	Alfa Aesar	Cat#A14594; CAS: 107-97-1
L-Alanine, ≥98%	Sigma-Aldrich, Merck	Cat#A7627; CAS: 56-41-7
Stachydrine HCl, 98%, (proline betaine)	Angene	Cat#AG00ILKM; CAS: 4136-37-2
L-Proline, 99%	Alfa Aesar	Cat#A10199; CAS: 147-85-3
Homomarine, ≥95%	Santa Cruz Biotechnology	Cat#sc-470671; CAS: 445-30-7
Trigonelline, 98%	Angene	Cat#AG003V2L; CAS: 6138-41-6

Nicotinic acid, ≥98%	Sigma-Aldrich, Merck	Cat#N4126; CAS: 59-67-6
Gonyol	Kindly provided by Kathleen Thume and Georg Pohnert; synthesized according to Gebser and Pohnert[50]	N/A
Sulfobetaine HCl, (DMSA, dimethylsulfonioacetate, dimethylthetin)	Toronto Research Chemicals	Cat#S699400; CAS: 4727-41-7
L-Cysteine, 98+%	Acros Organics	Cat#173600250; CAS: 52-90-4
Sodium methanthiolate, ≥90% (MeSH)	Sigma-Aldrich, Merck	Cat#71742; CAS: 5188-07-8
Methanol, ≥99.9%	Sigma-Aldrich, Merck	Cat#1060072500; CAS: 67-56-1
Glycine, 99%	Acros Organics	Cat#385900500; CAS: 56-40-6
L-Serine, 99%	Acros Organics	Cat#132660250; CAS: 56-45-1
L-Methionine, 98+%	Acros Organics	Cat#166160250; CAS: 63-68-3
DL-Methionine methylsulfonium Cl, 99%, (*S*-methylmethionine; SMM)	mcule	Cat#MCULE-1226059178; CAS: 3493-12-7
L-Homocysteine, 95%	Angene	Cat#AG0037FN CAS: 6027-13-0
IPTG	ORNAT	Cat#INA-1758-1400
Protease inhibitor Cocktail	Sigma-Aldrich, Merck	Cat#I3911
Strep-Tactin™ Sepharose™ Resin	IBA-Lifesciences	Cat#2-1201-010
D-Desthiobiotin	IBA-Lifesciences	Cat#2-1000-002
DL-Dithiothreitol (DTT)	Sigma-Aldrich, Merck	Cat#DO632; CAS: 3483-12-3
Cell Free Amino Acid Mixture - ^{13}C,^{15}N	Sigma-Aldrich, Merck	Cat#767964
β-Mercaptoethanol, 99%	Sigma-Aldrich, Merck	Cat#M3148 CAS: 60-24-2
n-Hexadecane, 99%	Alfa Aeser	Cat#A10322
Critical commercial assays, kits and consumables		
Miracloth	Sigma-Aldrich, Merck	Cat#475855
Spin-X® UF concentrators 500 µL, 10,000 MWCO	Corning	Cat#431478
mPAGE 4-20% Bis-Tris Precast Gel	Sigma-Aldrich, Merck	CatMP42G12
Buffer RLT	QIAGEN	Cat79216
Low Binding Silica Grinding Beads (100 µm)	Spex® SamplePrep	Cat2168
ISOLATE II RNA Mini Kit	Bioline, Meridian Bioscience	CatBIO-52072
TURBO™ DNase (2 U/µL)	Invitrogen, Thermo Fisher Scientific	Cat#AM2238
RNAClean XP magnetic beads	Beckman Coulter	Cat#A63987

Qubit™ RNA High Sensitivity (HS) Assay Kit	Invitrogen, Thermo Fisher Scientific	Cat#Q32852
Qubit™ 1X dsDNA High Sensitivity (HS) Assay Kit	Invitrogen, Thermo Fisher Scientific	Cat#Q33230
RNA ScreenTape Analysis	Agilent Technologies	Cat#5067-5576
High Sensitivity D1000 ScreenTape	Agilent Technologies	Cat#5067-5584
riboPOOL depletion kit with Pan-Bacteria probes	siTOOLs Biotech	Cat#dp-K024-000026
riboPOOL depletion kit with *E. huxleyi* probes	siTOOLs Biotech	Cat#dp-K024-000033
FastAP thermosensitive alkaline phosphatase, 1U/µl	Thermo Fisher Scientific	Cat#EF0651
RNA Clean & Concentrator-5 columns	Zymo Research	Cat#R1015
SuperScript™ IV First-Strand Synthesis System	Invitrogen, Thermo Fisher Scientific	Cat#18091200
T4 RNA ligase 1 (ssRNA Ligase), 30,000 U/ml	New England Biolabs	Cat#M0437M
T4 polynucleotide kinase (PNK), 10 U/µl	New England Biolabs	Cat#M0201S
RNase inhibitor, murine, 40 U/µl	New England Biolabs	Cat#M0314S
SUPERase-IN, 20 U/µl	Invitrogen, Thermo Fisher Scientific	Cat#AM2694
AccuPrime™ *Taq* DNA Polymerase, high fidelity	Invitrogen, Thermo Fisher Scientific	Cat#12346086
NovaSeq 6000 S1 Reagent Kit (100 cycles)	Illumina	Cat#20012865
NextSeq 500/550 Mid Output Kit v2.5 (150 Cycles)	Illumina	Cat#20024904
NucleoSpin Gel and PCR Clean-up Kit	MACHEREY-NAGEL	Cat#740609
Phusion High Fidelity DNA polymerase	Thermo Fisher Scientific	Cat#F530S
QIAprep Spin Miniprep Kit	QIAGEN	Cat#271040
Protein Assay Dye Reagent Concentrate	Bio Rad	Cat#5000006
Fluorometric Methionine Assay Kit	Sigma-Aldrich, Merck	Cat#MAK347
Millex®-GV Filter Unit (Sterile), pore size 0.22 µm	Millipore, Merck	Cat#SLGV033RS
Deposited data		
Co-culture RNA-sequencing reads (dual RNA-seq); demultiplexed, trimmed, QC filtered	This paper	BioProject: PRJNA976961
Lag phase RNA-sequencing reads; demultiplexed, trimmed, QC filtered	This paper	BioProject: PRJNA977030
Emiliania huxleyi CCMP3266 sGenome assembly	Sperfeld *et al.*[142]	https://zenodo.org/record/5702921 (Data S4)
Emiliania huxleyi CCMP3266 sGenome annotation version 2	This paper	https://weizmann.box.com/s/rr1hbu2zdnmfmnmia461ogspxdiib43e

Phaeobacter inhibens DSM 17395 genome assembly	Thole *et al.*[33]	assembly accession: GCA_000154765.2
Phaeobacter inhibens DSM 17395 genome annotations (RefSeq)	O'Leary *et al.*[143]	https://ftp.ncbi.nlm.nih.gov/genomes/refseq/bacteria/Phaeobacter_inhibens/latest_assembly_versions/GCF_000154765.2_ASM15476v2/
Phaeobacter inhibens DSM 17395 genome annotations (GenBank)	Thole *et al.*[33]	https://ftp.ncbi.nlm.nih.gov/genomes/genbank/bacteria/Phaeobacter_inhibens/latest_assembly_versions/GCA_000154765.2_ASM15476v2/
Phaeobacter inhibens DSM 17395 KEGG metabolic pathways annotation map	Kanehis and Goto[56]	https://www.genome.jp/pathway/pga01100 (pga01100)
Phaeobacter inhibens DSM 17395 BioCyc annotations (v27.0)	Karp *et al.*[144]	https://biocyc.org/organism-summary?object=GCF_000154765
Oligonucleotides		
1. *dmdA* KO upstream forward primer with homology to pCR™II-TOPO™: GTAACGGCCGCCAGTGTGCTGGAATTCGCCCTTGCCGCCGCATGGCAAACACCG	This paper	N/A
2. *dmdA* KO upstream reverse primer with homology to gentamycin cassette: GCATTACAGTTTACGAACCGAACAGGCTTATGTCAATCAGGTGCTCATGGTTTTGGCGGC	This paper	N/A
3. *dmdA* KO downstream forward primer with homology to gentamycin cassette: GGTGGGCTGCCCTTCCTGGTTGGCTTGGTTTCCGATGCAGTTTGCGTGGTGCG	This paper	N/A
4. *dmdA* KO downstream reverse primer with homology to pCR™II-TOPO™: CCGCCAGTGTGATGGATATCTGCAGAATTCGCCCTTCGCGCGTCGGCGATCTCTG	This paper	N/A
5. *dmdA* KO verification forward primer: GGACGCCATCGCGCTGAAC	This paper	N/A
6. *dmdA* KO verification reverse primer: GGCTGGCTTCTCATGATCTCGC	This paper	N/A
7. *bmt* KO upstream forward primer with homology to pCR™II-TOPO™: GTAACGGCCGCCAGTGTGCTGGAATTCGCCCTTGCGCGCTGGCGGGTGCTGC	This paper	N/A

8. *bmt* KO upstream reverse primer with homology to gentamycin cassette: GCATTACAGTTTACGAACCGAACAGGCTTATGTCAAGGGATGTTCCTGTGGGGGTGATATTC	This paper	N/A
9. *bmt* KO downstream forward primer with homology to gentamycin cassette: GGTGGGCTGCCCTTCCTGGTTGGCTTGGTTTCTCATGGACATAGCCCCAAGCCG	This paper	N/A
10. *bmt* KO downstream reverse primer with homology to pCR™II-TOPO™: CCGCCAGTGTGATGGATATCTGCAGAATTCGCCCTTGGCCCGGTCGTTGATTTCCTAC	This paper	N/A
11. *bmt* KO verification forward primer: CCGGCAGAACGGCGGGCATATCC	This paper	N/A
12. *bmt* KO verification reverse primer: GCTGGGGCGACCTGCGGGATTC	This paper	N/A
13. Gentamycin cassette forward primer: GTTGACATAAGCCTGTTCG	This paper	N/A
14. Gentamycin cassette reverse primer: GTTAGGTGGCGGTACTTGG	This paper	N/A
15. Gentamycin cassette verification forward primer: GTGCAAGCAGATTACGGTGACG	This paper	N/A
16. Gentamycin cassette verification reverse primer: GAGCCTACATGTGCGAATGATGC	This paper	N/A
17. *metE* KO upstream forward primer with homology to pCR™8/GW/TOPO: GTACAAAAAAGCAGGCTCCGAATTCGCCCTTAGCCTTCATCGACGCCCACAC	This paper	N/A
18. *metE* KO upstream reverse primer with homology to kanamycin cassette: GCATTACAGTTTACGAACCGAACAGGCTTATGTCAAGTGCCGAATCTCCTCAAGTCAG	This paper	N/A
19. *metE* KO downstream forward primer with homology to kanamycin cassette: GCCTTCTATCGCCTTCTTGACGAGTTCTTCTGACACCGCTCCTGCTGCTCCC	This paper	N/A
20. *metE* KO downstream reverse primer with homology to pCR™8/GW/TOPO: CTTTGTACAAGAAAGCTGGGTCGAATTCGCCCTGCCCCAATAGGCGCCAATGC	This paper	N/A
21. *metE* KO verification forward primer: CGGGGTGCGGGTTTGAAACC	This paper	N/A
22. *metE* KO verification reverse primer: GGGCCGATTGATCCGGCAATC	This paper	N/A
23. Kanamycin cassette forward primer: TTGACATAAGCCTGTTCGGTTCG	This paper	N/A
24. Kanamycin cassette reverse primer: TCAGAAGAACTCGTCAAGAAGGCG	This paper	N/A
25. Kanamycin cassette verification forward primer: GAGCACGTACTCGGATGGAA	This paper	N/A
26. Kanamycin cassette verification reverse primer: TTCCATCCGAGTACGTGCTC	This paper	N/A

27. Recombinant *mmuM* forward primer with homology to pET29b: CTTCTCAAATTGAGGATGACTCCATGCACTGCTTCGCGCTTTTAACGCGGC	This paper	N/A
28. Recombinant *mmuM* reverse primer with homology to pET29b: GTTTAACTTTAAGAAGGAGATATACATATGTCGCAGAATAATCCGTTACGCGCTC	This paper	N/A
29. pET29b forward primer with homology to *mmuM*: CAAGAAGAGCGCGTAACGGATTATTCTGCGACATATGTATATCTCCTTCTTAAAGTTAAAC	This paper	N/A
30. pET29b reverse primer with homology to *mmuM*: GCGGATATCGCCGCGTTAAAAGCGCGAAGCAGTGCATGGAGTCATCCTC	This paper	N/A
Recombinant DNA		
pDN12: *dmdA* KO plasmid (Upstream *dmdA*-Gm-Downstream *dmdA*-TOPOII)	This paper	N/A
pDN4: *bmt* KO plasmid (Upstream *bmt*-Gm-Downstream *bmt*-TOPOII)	This paper	N/A
pDN11: *metE* KO plasmid (Upstream *metE*-Km-Downstream *metE*-TOPO8)	This paper	N/A
pDN3: *bmt* expression vector (StrepTagII-*bmt*-pET29b)	This paper	Twist Biosciences
pDN10: *mmuM* expression vector (*mmuM*-StrepTagII-pET29b)	This paper	N/A
pBBR1MCS-5	Kovach *et al.*[145]	N/A
pYDR1	Abada *et al.*[45]	N/A
pCR™II-TOPO™	Invitrogen	Cat#K466040
pCR™8/GW/TOPO®	Invitrogen	Cat#K250020
Software and algorithms		
fastq-multx; v1.3.1	Aronesty[146]	https://github.com/brwnj/fastq-multx
Cutadapt; v1.18	Martin[147]	https://anaconda.org/bioconda/cutadapt
STAR; v2.7.5c	Dobin *et al.*[148]	https://github.com/alexdobin/STAR
featureCounts; v2.0.0	Liao *et al.*[149]	https://subread.sourceforge.net/
DeSeq2; v1.36.0	Love *et al.*[150]	https://bioconductor.org/packages/release/bioc/html/DESeq2.html
R; v4.2.0	R Core Team[151]	https://www.R-project.org/
ggplot2; v3.4.1	Wickham[152]	https://ggplot2.tidyverse.org
Growthcurver; v0.3.1	Sprouffske and Wagner[153]	https://github.com/sprouffske/growthcurver

multcomp; v1.4-23	Hothorn *et al.*[154]	https://cran.r-project.org/web/packages/multcomp/index.html
Compound Discoverer™ Software; v3.3	Thermo Fisher Scientific	Cat#OPTON-31061

Resource availability

Lead contact

Further information and requests for resources and reagents should be directed to and will be fulfilled by the lead contact, Einat Segev (Einat.Segev@weizmann.ac.il).

Materials availability

Plasmids generated in this study, as well as bacteria that are not deposited in public strain collections, will be made available on request.

Data and code availability

- RNA-sequencing data have been deposited at the NCBI Sequence Read Archive (SRA) and are publicly available as of the date of publication. Accession numbers are listed in the Key Resources Table. This paper analyses existing, publicly available genomic data. The accession numbers for the datasets are listed in the Key Resources Table.
- This paper does not report original code.
- Any additional information required to reanalyze the data reported in this paper is available from the lead contact upon request.

Experimental Model and Subject Details

Microalgae, media composition and general culture conditions

The algal strain *Emiliania huxleyi* CCMP3266 was purchased as an axenic culture from the National Center for Marine Algae and Microbiota (Bigelow Laboratory for Ocean Sciences, ME, USA). Absence of bacteria in axenic algal cultures was monitored periodically both by plating on ½ YTSS agar plates (yeast extract, 2 g/L; trypton, 1.25 g/L; sea salts, 20 g/L; agar, 16 g/L) and under the microscope. Algae were maintained in ASW_a medium (artificial seawater) at 18°C with a light/dark cycle of 18/6 h and an illumination intensity of

150 mmoles/m^2/s. The ASW_a medium was based on the protocol of Goyet and Poisson[155] and contained mineral salts (NaCl, 409.41 mM; Na_2SO_4, 28.22 mM; KCl, 9.08 mM; KBr, 0.82 mM; NaF, 0.07 mM; Na_2CO_3, 0.20 mM; $NaHCO_3$, 2 mM; MgCl · 6 H_2O, 50.66 mM; $CaCl_2$, 10.2 mM, $SrCl_2$ · 6 H_2O, 0.09 mM), f/2 vitamins (thiamine HCl, 100 µg/L; biotin, 0.5 µg/L; vitamin B_{12}, 0.5 µg/L), L1 trace elements (Na_2EDTA · $2H_2O$, 4.36 mg/L; $FeCl_3$ · $6H_2O$, 3.15 mg/L; $MnCl_2$ · $4H_2O$, 178.1 µg/L; $ZnSO_4$ · $7H_2O$, 23 µg/L; $CoCl_2$ · $6H_2O$, 11.9 µg/L; $CuSO_4$ · $5H_2O$, 2.5 µg/L; Na_2MoO_4 · $2H_2O$, 19.9 µg/L; H_2SeO3, 1.29 µg/L; $NiSO_4$ · $6H_2O$, 2.63 µg/L; Na_3VO_4, 1.84 µg/L; K_2CrO_4, 1.94 µg/L) and L1 nutrients ($NaNO_3$, 882 µM; NaH_2PO_4 · $2H_2O$, 36.22 µM). The components were dissolved in Milli-Q water (IQ 7003; Merck, Darmstadt, Germany) and the pH adjusted to 8.2 with HCl. Stock solutions of f/2 vitamins, L1 trace elements and L1 nutrients were purchased from the Bigelow Laboratory for Ocean Sciences (Boothbay, ME, USA).

Marine bacteria and media composition

The bacterial strain *Phaeobacter inhibens* DSM 17395 was purchased from the German Collection of Microorganism and Cell Cultures (DSMZ, Braunschweig, Germany). The bacterial strain *Sulfitobacter pontiacus* iR4 was isolated from a xenic culture of *Emiliania huxleyi* CCMP1516 (Beirales *et al*., *in revision*; the sequenced genome can be downloaded from zenodo[156]). The bacterial strains *Ruegeria* sp. DT77 and *Vibrio* sp. DT22 were isolated from the Mediterranean Sea and Red Sea, and have highest 16S rRNA nucleotide identity with *Ruegeria* sp. InAD-147 (accession: MF401348.1) and Vibrio sp. THAF190c (accession: CP045338.1), respectively[140]. The *Ruegeria* and *Vibrio* isolates belong to the Tawfik lab marine bacteria collection, which is now part of the Segev lab strain collection at the Weizmann Institute of Science, Israel. The marine bacteria were cultivated in ASW_b medium (identical to the ASW_a medium, but with additional 5 mM NH_4Cl and 33 mM Na_2SO_4; f/2 vitamins were omitted, and glucose added as indicated), filtered sea water medium (Mediterranean Sea water enriched with L1 trace elements, f/2 vitamins, and L1 nutrients in the same concentrations as used for ASW_a) or in ½ YTSS medium (yeast extract, 2 g/L; trypton, 1.25 g/L; sea salts; 20 g/L), as indicated. Bacterial isolates were kept at -80ºC in ½ YTSS medium with 20% glycerol for long-term storage.

Non-marine bacteria and media composition

The bacterial strains *Pantoea agglomerans* Pag2 and *Ewingella americana* EA were isolated from soil[141], and kindly provided by Jonathan Friedman (The Hebrew University of Jerusalem, Israel). The *Escherichia coli* strains DH5α, BL21 DE3 pLysS, K-12 MG1655, as well as the *Bacillus subtilis* strain 168 were obtained from the Bacteriology Unit of the Weizmann Institute of Science, Israel. The strains were cultivated in M9 medium (glucose, 3.6 g/L; Na_2HPO_4 ·

7H2O, 64 g/L; KH_2PO_4, 15 g/L; NH_4Cl, 5 g/L; NaCl, 2.5 g/L), LB medium (tryptone, 10 g/L; yeast extract, 5 g/L; NaCl, 10 g/L NaCl) or TYG medium (tryptone, 1 g/L; yeast extract, 1 g/L; glucose, 0.5 g/L; KCl, 6.34 g/L; NaCl, 1.20 g/L; $MgSO_4 \cdot 7H_2O$, 0.25 g/L; K_2HPO_4, 0.13 g/L; $CaCl_2 \cdot 2H_2O$, 0.22 g/L; K_2SO_4, 0.17 g/L; Na_2SO_4, 2.40 g/L; $NaHCO_3$, 0.50 g/L; Na_2CO_3, 0.09 g/L; Fe EDTA, 0.07 g/L), as indicated. Bacterial isolates were kept at -80ºC in LB medium with 20% glycerol for long-term storage.

Method Details

Co-culture RNA-sequencing: Experimental design

To analyze the transcriptome of *P. inhibens* DSM 17395 bacteria during co-cultivation with the *E. huxleyi* CCMP3266 algae, a dual RNA-sequencing approach was applied that allows probing prokaryotic and eukaryotic RNA in the same samples, without separating cells by e.g. filtration[157]. For cultivation, 250 mL Erlenmeyer flasks with 60 ml ASW_a medium were inoculated with either both organisms (co-cultures), or with one of the two organisms (pure cultures). Specifically, 24 replicate flasks were inoculated with co-cultures of algae and bacteria (20.000 *E. huxleyi* cells and 2.000 *P. inhibens* CFUs; bacteria were pre-cultivated for 48 h in ASW_b medium with 2 mM glucose and f/2 vitamins and added to algae four days after inoculation). Another 24 replicate flasks were inoculated with pure cultures of algae (20.000 *E. huxleyi* cells). All 48 flasks were sealed with aluminum foil and cultivated in standing cultures in a growth room at 18 ºC under a light/dark cycle of 16/8 hr. Illumination intensity during the light period was 150 mmoles/m^2/s. At each sampling point, three random flasks were sacrificed per condition and sampled to enumerate algal cells, bacterial colony forming units (CFU) and to harvest cells for RNA extraction (starting from day 0; see Supplement Figure S1 for sampling points). Nine additional replicate flasks were inoculated with pure cultures of bacteria (2.000 *P. inhibens* CFUs; 0.88 mM NH_4Cl and 2 mM glucose were added to the ASW_a medium to facilitate bacterial growth). The nine bacterial flasks were cultivated under the same conditions as the flasks with algae. Three flasks were repeatedly sampled to enumerate bacterial CFUs, while three flasks were sacrificed per sampling point to harvest cells for RNA extraction (see Supplement Figure S1 for growth curves and RNA sampling points).

Algal cell numbers were determined as technical triplicates using a CellStream flow cytometer (Merck, Darmstadt, Germany). Bacterial CFU numbers were determined as technical duplicates using serial plating on ½ YTSS medium agar plates. To harvest cells for RNA extraction, 50 mL culture was centrifuged for 5 min at 18 ºC and 3,220 g (5810 R swing-out centrifuge; Eppendorf, Hamburg, Germany) and the supernatant was removed by vacuum

suction. Cell pellets were resuspended in 450 µl RLT buffer (QIAGEN, Hilden, Germany) with 1% β-mercaptoethanol, transferred into a 2 mL screw cap tube with 300 mg of 100 µm acid washed Low Binding Silica Beads (SPEX SamplePrep, Metuchen, NJ, USA), plunged into liquid nitrogen and stored at -80 ºC for one month until use.

Co-culture RNA-sequencing: RNA extraction and library preparation

RNA extracts were generated from 30 selected cell pellets (3 biological replicates per sampling point) that originate from algal-bacterial co-cultures, axenic algae and bacteria grown in pure culture with 2 mM glucose (see Supplement Figure S1 for sampling points and sample designations). Cell pellets were disrupted by 5 min bead beating at 30 s^{-1} in a mixer mill MM 400 (Retsch, Haan, Germany). RNA was extracted from disrupted cells using the ISOLATE II RNA Mini Kit, which integrates a step for an on-column DNase treatment (Meridian Bioscience, OH, USA). The extracted RNA was subjected to a second DNAse treatment using the TURBO DNase kit (Thermo Fisher Scientific, Waltham, MA, USA) and subsequently purified with 2x concentrated RNAClean XP magnetic beads (Beckman Coulter, Brea, CA, USA). RNA quantity and integrity was evaluated with the Qubit RNA HS Assay (Invitrogen, Thermo Fisher Scientific, Waltham, MA, USA) and the Tapestation RNA ScreenTape analysis (Agilent Technologies, Santa Clara, CA, USA), respectively (Supplement Figure S2). Ribosomal RNA was depleted using the riboPOOL rRNA depletion kit in combination with Pan-Bacteria probes and custom probes generated for *E. huxleyi* rRNA from the nucleus, plastid and mitochondrion (siTOOLs Biotech, Planegg, Germany). For ribosomal RNA depletion, 0.9 µg of RNA was used as an input with 50 pmol of each of the two depletion probes. After rRNA depletion, RNA was purified with 2x concentrated RNAClean XP magnetic beads (Beckman Coulter, Brea, CA, USA). Subsequent library preparation was performed as described by Avraham *et al.*[157], which is a stranded, poly(A)-independent protocol that targets total RNA. Briefly, depleted RNA was fragmented by heat, treated with DNase and FastAP, and then 3'-tagged by ligating the barcoded adapters 1 to 30[157] (RNase-free HPLC purified; ordered from Integrated DNA Technologies, Coralville, IA, USA). After barcoding, we implemented a calibration sequencing run to quantify the relative abundance of bacterial RNA in each sample. This quantification allows to determine the optimal sample-specific sequencing depths, and prevents over-sequencing of samples that contain either dead algae, or only one of the two organisms. For the calibration RNA-sequencing run, we proceeded with half of the barcoded RNA and stored the rest at -80 ºC. All 30 samples were pooled in an equivolume and purified with RNA Clean & Concentrator-5 columns (Zymo Research, Irvine, CA, USA). RNA was reverse transcribed with the SuperScript IV First-Strand Synthesis System (Invitrogen, Thermo Fisher Scientific, Waltham, MA, USA), using the AR2 primer[157]. The resulting cDNA was 3'-ligated to the 3Tr3

adaptor[157] (HPLC purified; ordered from Integrated DNA Technologies, Coralville, IA, USA). The 3'-ligated cDNA was then amplified with 9 PCR cycles (see Supplement Figure S16A for PCR cycle optimization). Finally, the amplified cDNA was purified with a double-sided clean-up step (right: 0.5x, left: 1.5x; RNAClean XP beads, Beckman Coulter, Brea, CA, USA), followed by a left-sided clean-up step (0.7x). The size distribution of the final calibration sequencing library is shown in Supplement Figure S16B. After cleanup, the library was sequenced on a NextSeq 500 instrument with a 150 cycles Mid Output Kit (Illumina, San Diego, CA, USA) in paired-end mode (Read 1: 88 bp, Read 2: 78 bp, Index 1: 0 bp, Index 2: 0 bp). Sequencing data were analyzed for the relative abundance of algal and bacterial RNA per sample, using bioinformatics methods described in the section below. The library preparation protocol was then repeated for the final co-culture RNA-sequencing run, starting from the stored, barcoded RNA. The barcoded RNA was pooled in a way that co-culture samples with algae are expected to yield equal amounts of bacterial sequencing reads (Supplement Figure S1; co-culture day 04, 06 and 09; expected bacterial feature counts per sample: 250,000-500,000), while fewer sequencing reads were allocated to algal pure cultures (axenic day 04, 06, 09 and 11/12; expected algal feature counts per sample: 40,000,000), co-cultures with bleached algae (co-culture day 11/12; expected algal feature counts per sample: 25,000,000) and bacterial pure cultures (glucose 1 and glucose 2; expected bacterial feature counts per sample: 5,000,000). After reverse transcription and ligation, the 3'-ligated cDNA was amplified with 11 PCR cycles (see Supplement Figure S17A for PCR cycle optimization). The final co-culture RNA-sequencing library (Supplement Figure S17B) was deep-sequenced on a NovaSeq 6000 instrument with a 100 cycles S2 Kit (Illumina, San Diego, CA, USA) in paired-end mode (Read 1: 64 bp, Read 2: 54 bp, Index 1: 0 bp, Index 2: 0 bp; Supplement Table S1). The expected distribution of algal and bacterial sequencing reads per sample was confirmed as described below (see Supplement Table S2 for resulting algal and bacterial feature counts per sample).

Co-culture RNA-sequencing: Data analysis

Illumina raw reads were demultiplexed with fastq-multx[146], allowing one mismatch per barcode (v1.3.1; -m 1). Raw reads were then quality filtered and trimmed with cutadapt[147] (v1.18; -a AGATCGGAAGAGCACACGTCTGAACTCCAGTCAC -A AGATCGGAAGAGCGTCGTGTAGGGAAAGAGTGT -g T{20} -A A{20} --times 2 --nextseq-trim=20 -m 20 --pair-filter=both; see Supplement Table S2 for summary; reads where deposited under the BioProject accession: PRJNA976961). The quality filtered and trimmed reads were mapped to a reference fasta file that included the previously generated "synthetic genome" assembly (sGenome) of *E. huxleyi* CCMP3266[142] and the genome of *P. inhibens*

DSM 17395 (accession: GCF_000154765.2). Read mapping was conducted with STAR[148] (v2.7.5c; --outSAMattributes All --alignIntronMax 5000 --alignMatesGapMax 5000 --outSAMtype BAM SortedByCoordinate --outFilterMultimapNmax 100 --outSAMmultNmax 1). For compatibility with STAR, empty lines generated by cutadapt were replaced with N's (sed 's/^$/N/'). Reads that mapped to *E. huxleyi* features were counted using featureCounts from the subread package[149] (v2.0.0; -p -C -a Ehux3266_sGenome_v2.gff -F GTF -O --fraction; see Supplement Data S3 for annotation file). Of note, a slightly modified version of the previously generated *E. huxleyi* CCMP3266 annotation file was used with featureCounts[142], in which plastid and mitochondrion annotations were replaced by public annotations (accessions: JN022705.1 and JN022704.1, respectively). For compatibility with featureCounts, the NH:i attribute of STAR bam files was changed to "1" (sed -r 's/NH:i:[0-9]+/NH:i:1/g'; STAR reports the number of alternative alignments in the NH:i attribute, which interferes with featureCounts fractional counting). Reads that mapped to *P. inhibens* features were counted with the same featureCounts options but using the *P. inhibens* RefSeq annotations. The output of featureCounts is summarized in Supplement Table S2. To evaluate the efficiency of ribosomal RNA depletion, also non-rRNA features were summarized (Supplement Table S2), in which algal rRNA from the nucleus (*E. huxleyi* CCMP3266 sGenome gene ID: G8853), the plastid (Plas_rrn5, Plast_rrnL, Plast_rrnS) and the mitochondrion (Mito_rrnL, Mito_rrnS), as well as bacterial 23S rRNA (PGA1_RS00070, PGA1_RS12745, PGA1_RS14220, PGA1_RS16070), 16S rRNA (PGA1_RS00055, PGA1_RS12760, PGA1_RS14235, PGA1_RS16085) and 5S rRNA (PGA1_RS00075, PGA1_RS12740, PGA1_RS14215, PGA1_RS16065) were excluded.

Bacterial gene transcription was analyzed only in co-culture RNA-sequencing samples that contained *P. inhibens* (Supplement Table S2; Supplement Figure S1). Since sample-specific rRNA depletion efficiencies may skew results, bacterial rRNA features were removed from the feature count table for downstream analysis. To analyze sample variability, bacterial non-rRNA feature count results were normalized for sequencing depth and RNA composition using the DESeq2's median of ratios method, followed by a regularized log transformation and principle component analysis[150,158] (v1.36.0; blind = TRUE ; ntop = 500; R version 4.2.0; Supplement Figure S3). DESeq2 was further used to identify differentially expressed (DE) genes by comparing samples of bacteria growing with algae (co-culture day 04, 06 and 09; Supplement Figures S1 and S3) to samples of bacteria growing exponentially in pure cultures (glucose 1; Supplement Figures S1 and S3). The apglm method was used to shrink log2 fold changes and account for overweighing of features with low counts and high variability[159]. Shrunken log2 fold changes and adjusted *p*-values are given in the Supplement Data S1. To compare absolute transcript abundances between genes and samples, bacterial feature counts were

converted to transcripts per kilobase million (TPM); a normalization method that accounts for gene length and sequencing depth (Supplement Data S1). To identify the 20 highest transcribed metabolic genes, the *P. inhibens* feature table (Supplement Data S1) was filtered for genes that are part of the KEGG metabolic pathways annotation map[56] (pga01100; https://www.genome.jp/pathway/pga01100). The resulting 840 KEGG metabolic genes were filtered for the 20 genes with the highest mean transcript abundances in samples with algae (co-culture day 04, 06 and 09).

To identify methyl group metabolism genes in *P. inhibens*, publicly available functional annotations were added to the feature table (Supplement Data S1). These annotations include automatically generated NCBI RefSeq annotations[143], partially curated GenBank submitter annotations[33], KEGG annotations[56], as well as links to BioCyc[144] and the unifying UniProt Archive (UniParc[160]; links redirect to e.g. pre-computed domain annotations at the InterPro database[161]). Features of *P. inhibens* were then filtered for relevant genes, based on differential expression patterns (adjusted *p*-value: ≤ 0.5; log2 fold change: ≤ -0.585 and ≥ 0.585; Supplement Data S1). The DE-filtered genes were manually curated by sourcing the public annotations, which identified methyl group metabolism genes that are involved in transporting and catabolizing methylated compounds, in harvesting, dissimilating or assimilating one-carbon groups, or in synthesizing tetrahydrofolate (THF). Also genes that are involved in the ethylmalonyl-CoA pathway were included, which replenishes the TCA cycle by capturing CO_2 during growth on the methylated compound DMSP[99]. Complementary to this approach, methyl group metabolism genes were identified by revising literature on one-carbon metabolism[162,163], and searching for homologues genes in *P. inhibens* using nucleotide and protein BLAST[164]. In the latter approach, genes were considered as relevant if they exhibited ≥ 50 mean TPM in at least one of the sampling points. The resulting list, which includes 83 curated *P. inhibens* methyl group metabolism genes, is given in Supplement Table S3. For clarification, genes were excluded from the list that did not meet the above described cut-off filters, such as a putative DMSP cleavage enzyme (*dddP*; PGA1_RS09315) that was poorly transcribed in all samples (< 50 TPM), and non-regulated methyltransferases.

Growth response in bacteria to supplements

To test the effect of methylated compounds on the growth of *P. inhibens*, bacteria were streaked from glycerol stocks on ½ YTSS medium agar plates and incubated at 30 ºC for 48 hours. After incubation, a single colony was used to inoculate a pre-culture with 10 mL ASW_b medium (1 mM glucose, 100 mL Erlenmeyer flasks). The pre-culture was cultivated at 30 ºC with 130 rpm shaking for 48 hours. After 48 hours, the pre-culture was in the stationary phase and exhibited OD_{600} ≈ 0.1. The stationary phase pre-culture was used to inoculate the

main cultures (1 mL ASW_b medium, 1 mM glucose, start OD_{600} = 0.00001), which contained supplements as indicated (mainly 2 µM of a methylated compound; listed in Key Resources Table). Supplements were prepared as 50 mM stock solutions in Milli-Q water and sterilized by filtration with syringe filters (Millex-GV, 0.22 µm, PVDF, Merck, Darmstadt, Germany). Each inoculated main culture was divided into three or four different wells (replicates) of a 96-well microtiter plate (150 µl main culture per well) and overlaid with 50 µl hexadecane to prevent evaporation[165]. Cultivation of the main cultures was conducted at 30 ºC in an Infinite 200 Pro M Plex plate reader (Tecan Group Ltd., Männedorf, Switzerland) with alternating cycles of 4 min shaking and 16 min incubation. Absorption measurements were conducted at 600 nm following the shaking step.

The same growth protocol was used to analyze growth responses in *P. inhibens* KO mutants with deleted *dmdA* gene (Figure 3C), *bmt* gene (Figure 6A) or *metE* gene (Figure 6B), as well as in the marine wild-type bacteria *Vibrio* sp. DT22 (Figure 7A) and *Ruegeria* sp. DT77 (Supplement Figure S15A). A slightly modified protocol was used for *S. pontiacus* iR4 marine bacteria, in which ASW_b medium was replaced by filtered seawater medium (Supplement Figure S15B). To study the non-marine bacteria *P. agglomerans* Pag2, *E. americana* EA, *B. subtilis* 168, and *E. coli* strains BL21, DH5α and K-12, the growth protocol was modified as follows: cells were first pre-cultivated in LB medium until reaching stationary phase, and then transferred into main cultures with M9 medium at an initial OD_{600} = 0.00001. *Escherichia coli* strains were cultivated at 37 ºC (Figure 7 and Supplement Figure S15).

Growth data analysis

For data analysis, microtiter plate absorption values were converted into OD_{600} values by multiplying measured values with a factor of 3,8603. This factor was determined by comparing the absorption (at 600 nm) of a culture sample in a spectrophotometer using a 1 cm cuvette (Ultrospec 2100 Pro, Biochrom, Cambridge, UK) with the absorption in the microtiter plate reader (150 µl culture + 50 µl hexadecane per well). The background absorption, which is the mean absorption during the non-growth phase with stable OD_{600} values (≈ 2-8 hours), was subtracted from each individual well. Results were plotted in R (v4.2.0) using ggplot2 (v3.4.1). For visual aid, smoothing lines were added that average the replicates for each condition (geom_smooth; method: loess). Doubling times and lag times were calculated for each replicate using the Growthcurver package[153] (v0.3.1). For this package, background subtracted OD_{600} values were used as an input that span the time from the lowest to the highest measured absorptions. Growthcurver was used to fit the OD_{600} values into a logistic equation that describes the population size N_t (OD_{600}) at time t. The output of Growthcurver

includes the modelled growth rate r, the carrying capacity K, and the initial population size N_0.

$$N_t = \frac{K}{\left[1 + (\frac{K - N_0}{N_0}) \cdot e^{-r \cdot t}\right]}$$

To calculate lag times, we formulated a definition in which lag times equal the time t at which N_t (OD_{600}) reaches an absorption of 0.01. Using this definition, the logistic equation of Growthcurver was rearranged to t and solved with $N_t = 0.01$:

$$t = \left(-\frac{1}{r}\right) \cdot \left[\ln\left(\frac{K - N_t}{K - N_0}\right) - \ln\left(\frac{N_t}{N_0}\right)\right]$$

To calculate △lag times, we first determined the mean lag time for each condition. Then, the mean lag times of supplemented treatment conditions were subtracted from the mean lag time of the control condition. Thus, the resulting △lag times are a measure for the effect of supplements on the length of the lag phase. To determine the standard error of the difference between means σ_{M1-M2} , a formula was used that incorporates the sample variance σ and the number of replicates n per condition:

$$\sigma_{M1-M2} = \sqrt{\frac{\sigma_1^2}{n_1} + \frac{\sigma_2^2}{n_2}}$$

Doubling times were calculated by solving the logistic equation of Growthcurver with $N_t = 2N_0$. The R package multcomp[154] (v1.4-23) was used to identify significant differences between lag times and doubling times. Specifically, an ANOVA model (aov function) was fitted to the two growth parameters, followed by a Dunnett's test (glht function).

Knock-out mutants with deleted dmdA, bmt or metE gene

Primers and plasmids used to generate *P. inhibens* knock-out (KO) mutants are listed in the Key Resources Table. PCR amplification and restriction-free cloning[166] were performed using the Phusion High Fidelity DNA polymerase (Thermo Fisher Scientific, Waltham, MA, USA). PCR products were purified with the NucleoSpin Gel and PCR Clean-up kit (MACHEREY-NAGEL, Düren, Germany). Plasmids were purified with the QIAprep Spin Miniprep Kit (QIAGEN, Hilden, Germany).

To generate KO mutants for the *dmdA* gene (accession: PGA1_RS19020; gene 25) and the *bmt* gene (accession: PGA1_RS06660; gene 82), we first PCR-amplified ~1,000 bp upstream

and downstream regions of the respective loci (primers 1-4 for *dmdA*, and 7-10 for *bmt*). A gentamycin resistance gene was amplified from the plasmid pBBR1MCS-5 (primers 13-14). The PCR products (upstream region + gentamycin resistance + downstream region) were then assembled and cloned into the pCR™II-TOPO™ vector (Invitrogen, Thermo Fisher Scientific, Waltham, MA, USA) using restriction-free cloning[166]. This resulted in the KO plasmids pDN12 (*dmdA*) and pDN4 (*bmt*). For transformation, 10 µg of KO plasmid were added to 300 µl of competent *P. inhibens* cells (prepared by the method of Dower *et al.*[167]), and electroporated with a pulse of 2.5 kV (MicroPulser, Bio-Rad Laboratories, Hercules, CA, USA). Electroporated cells were recovered in 2 mL ½ YTSS medium for 12 hours at 30 ºC and transferred to selective ½ YTSS medium agar plates with 30 µg/ml gentamycin. To screen for transformants, single colonies were used as template for PCR reactions (primers 5-6 for *dmdA* KO mutants, primers 11-12 for *bmt* KO mutants, and primers 15-16 for both). Gene knock-outs were additionally verified in single-cell clones by Sanger sequencing.

To generate a *metE* KO mutant (accession: PGA1_RS13640; gene 65), the ~1,000 bp *metE* upstream and downstream regions were amplified with the primers 17-20. A selective kanamycin resistance gene was amplified from the plasmid pYDR1 (primers 23-24). Restriction-free cloning was conducted with the vector pCR™8/GW/TOPO® (Invitrogen, Thermo Fisher Scientific, Waltham, MA, USA), which resulted in the *metE* KO plasmid pDN11. Positive transformants were selected on ½ YTSS medium agar plates with 150 µg/ml kanamycin and PCR-verified with primers 21, 22, 25 and 26.

Stoichiometric calculations

To estimate the amount of methyl group requirements per *P. inhibens* cell during growth on glucose, we identified metabolites that are built from one-carbon (C1) groups[103,104], and are thus C1 sinks. The focus was on C1 sinks that are used as building blocks to construct macromolecules such as DNA, RNA and proteins, and for which quantitative data are available in *E. coli*[65]. We identified seven C1 sinks in *P. inhibens* (ATP, GTP, dATP, dGTP, dTTP, histidine and methionine; Supplement Table S4). Not included were serine, phosphatidylcholine, spermidine, macromolecule methylations and low abundant metabolites. Serine is an important C1 group donor in cells (Figure 1; gene 67), however, serine synthesis from glucose does not consume C1 groups. Phosphatidylcholine has a choline backbone with three *N*-methyl groups and is produced by many bacteria[168]. It was reported that some *Phaeobacter* species produce phosphatidylcholine[169], however, only minor amounts of this lipid were detected in *P. inhibens* DSM 17395 during growth with glucose[39]. The metabolite spermidine was excluded due to uncertainties about methyl group recycling. The bacterium *P. inhibens* possesses all genes required to synthesize spermidine by first decarboxylating *S*-

adenosylmethionine (SAM) to *S*-adenosyl 3-(methylsulfanyl)propylamine (dcSAM), and then condensing dcSAM with putrescine to spermidine (Figure 4A). Importantly, the *S*-methyl group of dcSAM is not directly incorporated into spermidine but remains attached to a side product of spermidine synthesis, which is *S*-methyl-5'-thioadenosine (MTA; Figure 4A). While the *S*-methyl group of MTA is recycled in other bacteria via the methionine salvage pathway, this pathway appears to be incomplete in *P. inhibens*. Thus, the incomplete methionine salvage pathway may result in the loss of one methyl group per synthesized spermidine molecule. However, considering that a yet unknown methionine salvage pathway may exist in *P. inhibens*[170], spermidine was not included as a C1 sink (Supplement Table S4). Methylated forms of the macromolecules DNA[105], RNA[106] and proteins[107] were also not included because to the best of our knowledge, no robust data exist on the quantity of macromolecule methylations in the cell. Lastly, not included were low-abundant C1 sinks such as pantothenate (required for CoA synthesis) or NAD/NADP, which represent negligible fractions of the bacterial biomass[65]. After identifying C1 sinks in *P. inhibens*, we gathered data on the amount of the respective sinks present in *E. coli* (Supplement Table S4). The values represent *E. coli* cells grown at 37 ºC in aerobic glucose minimal medium and at a doubling time of 40 min[65]. A single *E. coli* cell has a dry weight of 280 fg under these conditions, which we used to calculate the amount of C1 sinks present per cell (amol building block/cell; Supplement Table S4). We then multiplied the amount of C1 sinks per cell with the net amount of C1 groups that are incorporated into each of the sinks (amol C1 group/cell; Supplement Table S4). By summing up the results for the individual C1 sinks, we estimated that a single *E. coli* cell requires 190.1 amol C1 groups to synthesize its building blocks. To calculate the C1 group requirement per *P. inhibens* cell, we assumed that *P. inhibens* and *E. coli* produce the same amounts of the respective C1 sinks. This assumption is corroborated by the fact that *P. inhibens* is, like *E. coli*, a copiotrophic bacterium[41] with a single cell length of 1-2 µm[169]. To estimate ATP costs, we referred to experimentally determined data generated for *E. coli* cells grown with glucose[66]. Under this condition, *E. coli* has a growth costs of 59.81 mmol ATP per gram cells, and non-growth costs of 8.39 mmol ATP per gram cells and hour (dry weight). Based on a dry weight of 280 fg per cell[65], this equals 19,096 amol ATP per *E. coli* cell.

Lag phase RNA-sequencing

To analyze transcriptional changes induced by DMSP during the lag phase of *P. inhibens*, a glycerol stock of these bacteria was streaked on a ½ YTSS medium agar plate and incubated at 30 ºC for 48 hours. After incubation, a single colony was used to inoculate four pre-culture flasks, each containing 100 ml ASW_b medium with 1 mM glucose. The four pre-cultures were incubated for 48 hours (30 ºC, 130 rpm shaking), resulting in stationary phase bacteria

(OD_{600} ≈ 0.1). The stationary pre-cultures were then pooled and washed by centrifugation (5 min, 3,220 g and 4 ºC) using a 5810 R swing-out centrifuge (Eppendorf, Hamburg, Germany). After centrifugation, the supernatant was removed by vacuum suction, and pellets were re-suspended in ASW_b medium (without glucose). A second washing step was performed, after which pellets were resuspended in 30 mL ASW_b medium (without glucose) to concentrate the cells. The concentrated cells (OD_{600} = 0.82) were used to inoculate six main culture flasks with DMSP (50 µM) and six flasks without DMSP. Each flask contained 60 mL ASW_b medium (1 mM glucose, pre-warmed at 30 ºC, start OD_{600} = 0.01). The 12 inoculated main culture flasks were incubated at 30 ºC with 130 rpm shaking. Six flasks (three flasks with 50 µM DMSP and three flasks without DMSP) were harvested 15 min after inoculation for RNA extraction. The other six flasks were harvested 40 min after inoculation. Separate cultivation experiments were conducted to confirm that DMSP stimulates growth under the applied conditions (Supplement Figure S8). The protocol used for cell harvest and RNA extraction is described in the section *Co-culture RNA-sequencing: RNA extraction and library preparation* with the adaptation that cells were centrifuged at 4 ºC. Results of the RNA extraction are shown in Supplement Figure S9. All 12 extracted RNA samples were subjected to RNA library preparation as described in the same section, but with minor modifications. RNA fragmentation was conducted with 300 ng RNA per sample, and rRNA depletion was performed after the pooling step, using 100 pmol Pan-Bacteria probes. Of note, the 3'-ligated cDNA was amplified with 12 PCR cycles (see Supplement Figure S18A for PCR cycle optimization). The resulting lag phase RNA-sequencing library (Supplement Figure S18B) was sequenced on a NextSeq 500 instrument with a 150 cycles Mid Output Kit (Illumina, San Diego, CA, USA) in paired-end mode (Read 1: 89 bp, Read 2: 79 bp, Index 1: 0 bp, Index 2: 0 bp; Supplement Table S5 and S6).

The pipeline described in the section *Co-culture RNA-sequencing: Data analysis* was used to analyze lag phase RNA-sequencing data. Quality filtered and trimmed sequencing reads (deposited under the BioProject accession: PRJNA977030) were mapped to a reference fasta file that contained only the genome of *P. inhibens* DSM 17395 (accession: GCF_000154765.2). After generating the *P. inhibens* non-rRNA feature count table, the data was used as input with the DESeq2 PCA plot function to confirm close clustering of replicates (Supplement Figure S10). DESeq2 was also used to compare gene expression in DMSP-supplemented samples with control samples 15 min and 40 min after inoculation (Supplement Figure S11). The DE results were included in the TPM normalized non-RNA feature table (Supplement Data S2).

Lag phase LC-MS analysis with [^{13}C-methyl]DMSP

To analyze DMSP methyl group assimilation during the lag phase, [^{13}C-methyl]DMSP, which contained two ^{13}C-labeled methyl groups, was synthesized in the Organic Synthesis Unit, Chemical Research Support, Weizmann Institute of Science, Israel. Labeled [^{13}C-methyl]DMSP was prepared according to Dickschat *et al.*[171]. The synthesis was carried out by the acid-catalysed addition of [$^{13}C_2$]dimethyl sulfide to acrylic acid, using the experimental conditions described in the literature for the deuterium labelled compound. The ^{13}C-labelling was confirmed by ^{1}H NMR, based on the appearance of the methyl signals as a doublet centered at δ = 3 ppm, the typical ^{1}H-^{13}C J coupling constant of 145 Hz and the mass spectrum showing the molecular ion at *m/z* 137. The NMR and the mass spectra did not show a signal for unlabelled DMSP.

Growth conditions for experiments with [^{13}C-methyl]DMSP were comparable to those applied for lag phase RNA-sequencing. Briefly, pre-cultures of *P. inhibens* were cultivated for 48 h (100 ml ASW_b medium, 1 mM glucose) and washed twice by centrifugation. A concentrated pre-culture pool of stationary phase bacteria was used to inoculate eight main culture flasks (60 ml ASW_b medium, 1 mM glucose; start OD_{600} = 0.01)—four flasks contained 50 µM [^{13}C-methyl]DMSP and four flasks contained 50 µM non-labeled DMSP. The eight main culture flasks were harvested 2 hours after inoculation by centrifugation (10 min, 7.000 rpm, 4º C; see Supplement Figure S8 for growth curves), and cell pellets were subsequently snap-frozen in liquid nitrogen.

Extraction and analysis of polar metabolites were performed as previously described in Malitsky *et al.*[172] and Zheng *et al.*[173] with some modifications. The bacterial pellets were extracted with 1 mL of a pre-cooled (-20˚C) homogenous methanol:methyl-tert-butyl-ether (MTBE) 1:3 (v/v) mixture. The tubes were vortexed and sonicated for 30 min in an ice-cold sonication bath (taken for a brief vortex every 10 min). Then, 0.5 mL of a UPLC-grade water:methanol (3:1, v/v) solution with 1:500 diluted ^{13}C- and ^{15}N-labeled amino acids standard mix (Sigma-Aldrich, Merck, Darmstadt, Germany) was added to the tubes, followed by vortex and centrifugation. The upper organic phase was discarded. The polar phase was re-extracted with 0.5 mL of MTBE. The lower polar phase was then dried under a gentle stream of nitrogen and kept at -80˚C for metabolite analysis. Dry polar samples were re-suspended in 80 µL Methanol:DDW (50:50) and centrifuged twice to remove the debris. The resuspended samples (40 µL) were transferred to HPLC vials for injection.

LC-MS metabolic profiling was done as described by Zheng *et al.*[173] with minor modifications. Briefly, analysis was performed using an Acquity I class UPLC System combined with a Q

Exactive Plus Orbitrap™ mass spectrometer (Thermo Fisher Scientific, Waltham, USA), operated in a positive and negative ionization modes. The LC separation was done using a SeQuant Zic-pHilic column (150 mm × 2.1 mm) with a SeQuant guard column (20 mm × 2.1 mm; Merck, Darmstadt, Germany). The mobile phase B contained acetonitrile, and the mobile phase A contained 20 mM ammonium carbonate with 0.1% ammonia hydroxide in water:acetonitrile (80:20, v/v). The flow rate was kept at 200 µL/min and the gradient was as follows: 0-2 min 75% of B, 14 min 25% of B, 18 min 25% of B, 19 min 75% of B, for 4 min, 23 min 75% of B. Data processing was done using the Compound Discoverer software (v3.3; Thermo Fisher Scientific, Waltham, USA), when detected compounds were identified by accurate mass, retention time, isotope pattern, and fragments. The software reports the fractional label incorporation (exchange rate) after natural abundance correction for each compound. LC-MS data were manually searched for metabolites involved in methyl group metabolism. This included DMSP, 3-*S*-methylmercaptopropionate (3-MMPA), *S*-adenosylmethionine (SAM), *S*-adenosyl 3-(methylsulfanyl)propylamine (dcSAM), *S*-methyl-5'-thioadenosine (MTA), methionine, serine, glycine, 5-methyltetrahydrofolate, 5,10-methylenetetrahydrofolate, 5,10-methenyltetrahydrofolate, N^{10}-formyltetrahydrofolate, thymidine-5'-phosphate (dTMP), *S*-methyl-5-thio-D-ribofuranose, *S*-methyl-5-thio-α-D-ribose 1-phosphate (1-PMTR), *S*-Methyl-5-thio-D-ribulose 1-phosphate and ATP. The manual search confirmed the presence of labeled DMSP, SAM and MTA, which were identified by the MS2 fragmentation patterns.

Methionine synthesis with cell crude extracts

Enzymatic methionine synthesis was measured in cell crude extracts using a method adapted from published protocols[174,175]. A glucose-grown pre-culture was used to inoculate four main culture flasks (100 ml ASW_b medium, 5.5 mM glucose). The main cultures were then cultivated for four days (30 ºC, 130 rpm) until reaching stationary phase (OD_{600} ≈ 1.0). Two stationary main culture flasks were incubated for 2 hours with 1 µM DMSP (30 ºC, 130 rpm), while the other two flasks were kept as untreated controls. After 2 hours of incubation, cells were harvested by centrifugation (5 min, 3,220 g, 4 ºC), and pellets were resuspended in 1 mL Solution A (50 mM Hepes-KOH, pH 7.5; all steps were conducted on ice, using pre-cooled solutions at 4 ºC). Resuspended cells were then washed twice by centrifugation (5 min, 15,000 g, 4 ºC), and resuspended in 1 mL Solution B (50 mM Hepes-KOH, pH 7.5, 10 mM β-mercaptoethanol, 1 mM EDTA). To disintegrate cell membranes, cells were transferred into 2 mL screw-capped tubes filled with 300 mg of 100 µm acid-washed Low Binding Silica Beads (SPEX SamplePrep, Metuchen, NJ, USA), plunged into liquid nitrogen, thawed, and disrupted by 5 min bead beating at 30 s^{-1} in a mixer mill MM 400 (Retsch, Haan, Germany). Disrupted

cells were centrifuged (5 min, 15,000 g, 4 ºC) and the supernatant transferred into a new tube, resulting in the cell crude extract. Protein concentrations were measured using the Protein Assay Dye Reagent Concentrate (Bio-Rad Laboratories, Hercules, CA, USA). Enzymatic reactions were performed by mixing 0.5 mL cell crude extract (1 mg protein/mL) with 0.5 mL solution C (60 mM potassium-phosphate buffer, pH 7.5, 4.5 mM homocysteine and 4.5 mM DMSP). The reaction mixes were incubated for 1 hour at 37 ºC. After incubation, 500 µl of the enzymatic reactions were transferred into fresh tubes, plunged in liquid nitrogen, and lyophilized for subsequent metabolite extraction and LC-MS analysis, as described in the section *Lag phase LC-MS analysis with [13C-methyl]DMSP* (but in negative ionization mode). The identification of methionine and 3-MMPA was confirmed by using authentic standards.

Heterologous expression of Bmt

Primers and plasmids used for heterologous expression of Bmt and MmuM (positive control) are listed in the Key Resources Table. To produce *P. inhibens* Bmt (accession: PGA1_RS06660), a pET29b expression vector was designed that encodes the *bmt* gene together with an N-terminal Strep-tag II peptide sequence (pDN3). The vector was synthesized by Twist Biosciences (San Francisco, CA, USA). To produce *E. coli* MmuM (accession: Q47690), the respective gene was PCR-amplified from *E. coli* K-12 MG1655 (primers 27-28). The expression vector was PCR-amplified from pET29b (primers 29-30) and cloned together with the *mmuM* PCR product using the CPEC technique[176]. This resulted in a MmuM expression vector with C-terminally fused Strep-tag II (pDN10). Plasmid construction was validated by Sanger sequencing. *E. coli* BL21 competent cells were transformed by electroporation with 100 µg expression vector, using a pulse of 1.8 kV (MicroPulser, Bio-Rad Laboratories, Hercules, CA, USA). Electroporated cells were selected for positive transformants using LB medium agar plates with 50 µg/ml kanamycin. For protein expression, *E. coli* BL21 transformants were grown in TYG medium with 50 µg/ml kanamycin at 37ºC until reaching the mid-log phase (OD_{600} = 0.7). Protein expression was induced by adding 0.2 mM IPTG. Cells were harvested three hours after IPTG induction by centrifugation (4,000 rpm, 15 min, 4 °C). Cell pellets were resuspended in 20 mL NP buffer (50 mM NaH_2PO_4, 300 mM NaCl, pH 8) with 100 µl 10X Protease Inhibitor Cocktail (Sigma-Aldrich, Merck, Darmstadt, Germany). Resuspended cells were filtered with Miracloth (Sigma-Aldrich, Merck, Darmstadt, Germany) and passed three times through a French Pressure cell press (15,000 psi) for cell disruption. Disrupted cells were centrifuged (4,000 rpm, 15min, 4 °C) and the supernatant was loaded onto a Strep-Tactin Sepharose resin column (IBA-Lifesciences, Göttingen, Germany). The column was washed three times with 5 mL NP buffer, and proteins were eluted with 3 mL NPD buffer (50 mM NaH_2PO_4, 300 mM NaCl, 2.5 mM Desthibiotin, pH 8). Eluted proteins were

concentrated with a 10 kDa membrane (Spin-X® UF 500 µL Centrifugal Concentrator, 10,000 MWCO; Corning, NY, USA) in 20 mM HEPES-KOH buffer (pH 7.5). Protein concentrations were determined using the Protein Assay Dye Reagent Concentrate (Bio-Rad Laboratories, Hercules, CA, USA). The purity was controlled by electrophoresing 3 µg of protein with SDS-sample buffer on a polyacrylamide gel (mPAGE™ 4-20% Bis-Tris Precast Gel, Merck, Darmstadt, Germany), followed by Bio-Safe Coomassie staining (Bio-Rad Laboratories, Hercules, CA, USA; Supplement Figure S14).

Methionine synthesis with purified Bmt

Methionine synthesis with different methyl group donors was measured *in vitro*, using purified enzyme and a protocol adapted from Ranocha *et al.*[177]. The *in vitro* reactions contained buffer (20 mM HEPES-KOH, pH 7.5, 2 mM dithiothreitol), a methyl group acceptor (2 mM homocysteine), a methyl group donor (200 µM of either DMSP, betaine or SMM) and purified enzyme (200 µM of either Bmt or MmuM). The *in vitro* reactions (v = 50 µl) were incubated for 2 hours at 30 ºC. Methionine synthesis was measured using the Methionine Assay Kit (Sigma-Aldrich, Merck, Darmstadt, Germany). For measurements, 20 µl of each *in vitro* reaction was mixed with 30 µl Met Assay Buffer and 50 µl Met Assay Reaction Mix. In parallel, 20 µl of the same *in vitro* reactions were mixed with 30 µl Met Assay Buffer and 50 µl Met Assay Background Control Mix. The mixes were incubated for 30 min at 37 ºC, followed by fluorescence readings (λ_{ex} = 535 nm/λ_{em} = 587 nm; Infinite 200 Pro M Plex plate reader, Tecan Group Ltd., Männedorf, Switzerland). The Methionine Assay Kit includes a methionine standard for absolute quantifications. The steps needed to produce purified proteins and to measure enzymatic methionine formation were repeated in three independent experiments.

Supplemental information titles and legends

References

1. Buchan, A., LeCleir, G.R., Gulvik, C.A., and González, J.M. (2014). Master recyclers: features and functions of bacteria associated with phytoplankton blooms. Nat Rev Microbiol *12*, 686–698. 10.1038/nrmicro3326.

2. Cole, J.J., Findlay, S., and Pace, M.L. (1988). Bacterial production in fresh and saltwater ecosystems: a cross-system overview. Marine Ecology Progress Series *43*, 1–10.

3. Ducklow, H.W., Kirchman, D.L., Quinby, H.L., Carlson, C.A., and Dam, H.G. (1993). Stocks and dynamics of bacterioplankton carbon during the spring bloom in the eastern North

Atlantic Ocean. Deep Sea Research Part II: Topical Studies in Oceanography *40*, 245–263. 10.1016/0967-0645(93)90016-G.

4. Field, C.B., Behrenfeld, M.J., Randerson, J.T., and Falkowski, P. (1998). Primary production of the biosphere: integrating terrestrial and oceanic components. Science *281*, 237–240. 10.1126/science.281.5374.237.

5. Johnsen, G., Leu, E., and Gradinger, R. (2020). Marine micro- and macroalgae in the polar night. In Polar night marine ecology Advances in Polar Ecology., J. Berge, G. Johnsen, and J. H. Cohen, eds. (Springer International Publishing), pp. 67–112. 10.1007/978-3-030-33208-2_4.

6. Caporaso, J.G., Paszkiewicz, K., Field, D., Knight, R., and Gilbert, J.A. (2012). The Western English Channel contains a persistent microbial seed bank. ISME J *6*, 1089–1093. 10.1038/ismej.2011.162.

7. Lennon, J.T., and Jones, S.E. (2011). Microbial seed banks: the ecological and evolutionary implications of dormancy. Nat Rev Microbiol *9*, 119–130. 10.1038/nrmicro2504.

8. Sebastián, M., Estrany, M., Ruiz-González, C., Forn, I., Sala, M.M., Gasol, J.M., and Marrasé, C. (2019). High growth potential of long-term starved deep ocean opportunistic heterotrophic bacteria. Frontiers in Microbiology *10*. 10.3389/fmicb.2019.00760.

9. Kjelleberg, S., Albertson, N., Flärdh, K., Holmquist, L., Jouper-Jaan, Å., Marouga, R., Östling, J., Svenblad, B., and Weichart, D. (1993). How do non-differentiating bacteria adapt to starvation? Antonie van Leeuwenhoek *63*, 333–341. 10.1007/BF00871228.

10. Finkel, S.E. (2006). Long-term survival during stationary phase: evolution and the GASP phenotype. Nature Reviews Microbiology *4*, 113–120. 10.1038/nrmicro1340.

11. Cappello, S., Denaro, R., Giuliano, L., and Yakimov, M.M. (2008). Persistence of *Alteromonas* genus during a long-term starvation in a marine microcosm. Ann. Microbiol. *58*, 15–20. 10.1007/BF03179439.

12. Needham, D.M., and Fuhrman, J.A. (2016). Pronounced daily succession of phytoplankton, archaea and bacteria following a spring bloom. Nat Microbiol *1*, 1–7. 10.1038/nmicrobiol.2016.5.

13. Ferrer-González, F.X., Widner, B., Holderman, N.R., Glushka, J., Edison, A.S., Kujawinski, E.B., and Moran, M.A. (2021). Resource partitioning of phytoplankton metabolites that support bacterial heterotrophy. ISME J *15*, 762–773. 10.1038/s41396-020-00811-y.

14. Kieft, B., Li, Z., Bryson, S., Hettich, R.L., Pan, C., Mayali, X., and Mueller, R.S. (2021). Phytoplankton exudates and lysates support distinct microbial consortia with specialized metabolic and ecophysiological traits. Proceedings of the National Academy of Sciences *118*, e2101178118. 10.1073/pnas.2101178118.

15. Lempp, M., Lubrano, P., Bange, G., and Link, H. (2020). Metabolism of non-growing bacteria. Biological Chemistry *401*, 1479–1485. 10.1515/hsz-2020-0201.

16. Dworkin, J., and Harwood, C.S. (2022). Metabolic reprogramming and longevity in quiescence. Annual Review of Microbiology *76*, 91–111. 10.1146/annurev-micro-041320-111014.

17. Jacob, F., and Monod, J. (1961). Genetic regulatory mechanisms in the synthesis of proteins. Journal of Molecular Biology *3*, 318–356. 10.1016/S0022-2836(61)80072-7.

18. Bertrand, R.L. (2019). Lag phase is a dynamic, organized, adaptive, and evolvable period that prepares bacteria for cell division. Journal of Bacteriology *201*, e00697-18. 10.1128/JB.00697-18.

19. Larsen, N., Boye, M., Siegumfeldt, H., and Jakobsen, M. (2006). Differential expression of proteins and genes in the lag phase of *Lactococcus lactis* subsp. *lactis* grown in synthetic medium and reconstituted skim milk. Applied and Environmental Microbiology *72*, 1173–1179. 10.1128/AEM.72.2.1173-1179.2006.

20. Rolfe, M.D., Rice, C.J., Lucchini, S., Pin, C., Thompson, A., Cameron, A.D.S., Alston, M., Stringer, M.F., Betts, R.P., Baranyi, J., et al. (2012). Lag phase is a distinct growth phase that prepares bacteria for exponential growth and involves transient metal accumulation. Journal of Bacteriology *194*, 686–701. 10.1128/JB.06112-11.

21. Madar, D., Dekel, E., Bren, A., Zimmer, A., Porat, Z., and Alon, U. (2013). Promoter activity dynamics in the lag phase of *Escherichia coli*. BMC Systems Biology *7*, 136. 10.1186/1752-0509-7-136.

22. Sekar, K., Rusconi, R., Sauls, J.T., Fuhrer, T., Noor, E., Nguyen, J., Fernandez, V.I., Buffing, M.F., Berney, M., Jun, S., et al. (2018). Synthesis and degradation of FtsZ

quantitatively predict the first cell division in starved bacteria. Molecular Systems Biology *14*, e8623. 10.15252/msb.20188623.

23. Basan, M., Honda, T., Christodoulou, D., Hörl, M., Chang, Y.-F., Leoncini, E., Mukherjee, A., Okano, H., Taylor, B.R., Silverman, J.M., et al. (2020). A universal trade-off between growth and lag in fluctuating environments. Nature *584*, 470–474. 10.1038/s41586-020-2505-4.

24. Cooper, M.B., and Smith, A.G. (2015). Exploring mutualistic interactions between microalgae and bacteria in the omics age. Current Opinion in Plant Biology *26*, 147–153. 10.1016/j.pbi.2015.07.003.

25. D'Souza, G., Shitut, S., Preussger, D., Yousif, G., Waschina, S., and Kost, C. (2018). Ecology and evolution of metabolic cross-feeding interactions in bacteria. Nat. Prod. Rep. *35*, 455–488. 10.1039/C8NP00009C.

26. Fritts, R.K., McCully, A.L., and McKinlay, J.B. (2021). Extracellular metabolism sets the table for microbial cross-feeding. Microbiol Mol Biol Rev *85*, e00135-20. 10.1128/MMBR.00135-20.

27. Simon, M., Scheuner, C., Meier-Kolthoff, J.P., Brinkhoff, T., Wagner-Döbler, I., Ulbrich, M., Klenk, H.-P., Schomburg, D., Petersen, J., and Göker, M. (2017). Phylogenomics of *Rhodobacteraceae* reveals evolutionary adaptation to marine and non-marine habitats. ISME J *11*, 1483–1499. 10.1038/ismej.2016.198.

28. González, J.M., and Moran, M.A. (1997). Numerical dominance of a group of marine bacteria in the alpha-subclass of the class Proteobacteria in coastal seawater. Applied and Environmental Microbiology *63*, 4237–4242. 10.1128/aem.63.11.4237-4242.1997.

29. Luo, H., and Moran, M.A. (2014). Evolutionary ecology of the marine Roseobacter clade. Microbiology and Molecular Biology Reviews *78*, 573–587. 10.1128/MMBR.00020-14.

30. Brinkhoff, T., Bach, G., Heidorn, T., Liang, L., Schlingloff, A., and Simon, M. (2004). Antibiotic production by a *Roseobacter* clade-affiliated species from the German Wadden Sea and its antagonistic effects on indigenous isolates. Applied and Environmental Microbiology *70*, 2560–2565. 10.1128/AEM.70.4.2560-2565.2003.

31. Zech, H., Thole, S., Schreiber, K., Kalhöfer, D., Voget, S., Brinkhoff, T., Simon, M., Schomburg, D., and Rabus, R. (2009). Growth phase-dependent global protein and metabolite

profiles of *Phaeobacter gallaeciensis* strain DSM 17395, a member of the marine *Roseobacter*-clade. PROTEOMICS *9*, 3677–3697. 10.1002/pmic.200900120.

32. Seyedsayamdost, M.R., Case, R.J., Kolter, R., and Clardy, J. (2011). The Jekyll-and-Hyde chemistry of *Phaeobacter gallaeciensis*. Nature Chem *3*, 331–335. 10.1038/nchem.1002.

33. Thole, S., Kalhoefer, D., Voget, S., Berger, M., Engelhardt, T., Liesegang, H., Wollherr, A., Kjelleberg, S., Daniel, R., Simon, M., et al. (2012). *Phaeobacter gallaeciensis* genomes from globally opposite locations reveal high similarity of adaptation to surface life. ISME J *6*, 2229–2244. 10.1038/ismej.2012.62.

34. Drüppel, K., Hensler, M., Trautwein, K., Koßmehl, S., Wöhlbrand, L., Schmidt-Hohagen, K., Ulbrich, M., Bergen, N., Meier-Kolthoff, J.P., Göker, M., et al. (2014). Pathways and substrate-specific regulation of amino acid degradation in *Phaeobacter inhibens* DSM 17395 (archetype of the marine *Roseobacter* clade). Environmental Microbiology *16*, 218–238. 10.1111/1462-2920.12276.

35. Wiegmann, K., Hensler, M., Wöhlbrand, L., Ulbrich, M., Schomburg, D., and Rabus, R. (2014). Carbohydrate catabolism in *Phaeobacter inhibens* DSM 17395, a member of the marine *Roseobacter* clade. Applied and Environmental Microbiology *80*, 4725–4737. 10.1128/AEM.00719-14.

36. Segev, E., Wyche, T.P., Kim, K.H., Petersen, J., Ellebrandt, C., Vlamakis, H., Barteneva, N., Paulson, J.N., Chai, L., Clardy, J., et al. (2016). Dynamic metabolic exchange governs a marine algal-bacterial interaction. eLife *5*, e17473. 10.7554/eLife.17473.

37. Wienhausen, G., Noriega-Ortega, B.E., Niggemann, J., Dittmar, T., and Simon, M. (2017). The exometabolome of two model strains of the *Roseobacter* group: a marketplace of microbial metabolites. Frontiers in Microbiology *8*. 10.3389/fmicb.2017.01985.

38. Freese, H.M., Methner, A., and Overmann, J. (2017). Adaptation of surface-associated bacteria to the open ocean: a genomically distinct subpopulation of *Phaeobacter gallaeciensis* colonizes pacific mesozooplankton. Frontiers in Microbiology *8*. 10.3389/fmicb.2017.01659.

39. Trautwein, K., Hensler, M., Wiegmann, K., Skorubskaya, E., Wöhlbrand, L., Wünsch, D., Hinrichs, C., Feenders, C., Müller, C., Schell, K., et al. (2018). The marine bacterium *Phaeobacter inhibens* secures external ammonium by rapid buildup of intracellular nitrogen stocks. FEMS Microbiology Ecology *94*, fiy154. 10.1093/femsec/fiy154.

40. Dittmann, K.K., Sonnenschein, E.C., Egan, S., Gram, L., and Bentzon-Tilia, M. (2019). Impact of *Phaeobacter inhibens* on marine eukaryote-associated microbial communities. Environmental Microbiology Reports *11*, 401–413. 10.1111/1758-2229.12698.

41. Wünsch, D., Trautwein, K., Scheve, S., Hinrichs, C., Feenders, C., Blasius, B., Schomburg, D., and Rabus, R. (2019). Amino acid and sugar catabolism in the marine bacterium *Phaeobacter inhibens* DSM 17395 from an energetic viewpoint. Applied and Environmental Microbiology *85*, e02095-19. 10.1128/AEM.02095-19.

42. Bramucci, A.R., and Case, R.J. (2019). *Phaeobacter inhibens* induces apoptosis-like programmed cell death in calcifying *Emiliania huxleyi*. Sci Rep *9*, 5215. 10.1038/s41598-018-36847-6.

43. Koblitz, J., Will, S.E., Riemer, S.A., Ulas, T., Neumann-Schaal, M., and Schomburg, D. (2021). The metano modeling toolbox MMTB: an intuitive, web-based toolbox introduced by two use cases. Metabolites *11*, 113. 10.3390/metabo11020113.

44. Henriksen, N.N.S.E., Lindqvist, L.L., Wibowo, M., Sonnenschein, E.C., Bentzon-Tilia, M., and Gram, L. (2022). Role is in the eye of the beholder—the multiple functions of the antibacterial compound tropodithietic acid produced by marine Rhodobacteraceae. FEMS Microbiology Reviews *46*, fuac007. 10.1093/femsre/fuac007.

45. Abada, A., Beiralas, R., Narvaez, D., Sperfeld, M., Duchin-Rapp, Y., Lipsman, V., Yuda, L., Cohen, B., Carmieli, R., Ben-Dor, S., et al. (2023). Aerobic bacteria produce nitric oxide via denitrification and promote algal population collapse. ISME J, 1–17. 10.1038/s41396-023-01427-8.

46. Thøgersen, M.S., Melchiorsen, J., Ingham, C., and Gram, L. (2018). A novel microbial culture chamber co-cultivation system to study algal-bacteria interactions using *Emiliania huxleyi* and *Phaeobacter inhibens* as model organisms. Frontiers in Microbiology *9*. 10.3389/fmicb.2018.01705.

47. Zech, H., Hensler, M., Koßmehl, S., Drüppel, K., Wöhlbrand, L., Trautwein, K., Hulsch, R., Maschmann, U., Colby, T., Schmidt, J., et al. (2013). Adaptation of *Phaeobacter inhibens* DSM 17395 to growth with complex nutrients. PROTEOMICS *13*, 2851–2868. 10.1002/pmic.201200513.

48. Blunden, G., Smith, B.E., Irons, M.W., Yang, M.-H., Roch, O.G., and Patel, A.V. (1992). Betaines and tertiary sulphonium compounds from 62 species of marine algae. Biochemical Systematics and Ecology *20*, 373–388. 10.1016/0305-1978(92)90050-N.

49. Keller, M.D., Kiene, R.P., Matrai, P.A., and Bellows, W.K. (1999). Production of glycine betaine and dimethylsulfoniopropionate in marine phytoplankton. I. Batch cultures. Marine Biology *135*, 237–248. 10.1007/s002270050621.

50. Gebser, B., and Pohnert, G. (2013). Synchronized regulation of different zwitterionic metabolites in the osmoadaption of phytoplankton. Marine Drugs *11*, 2168–2182. 10.3390/md11062168.

51. Galí, M., Devred, E., Levasseur, M., Royer, S.-J., and Babin, M. (2015). A remote sensing algorithm for planktonic dimethylsulfoniopropionate (DMSP) and an analysis of global patterns. Remote Sensing of Environment *171*, 171–184. 10.1016/j.rse.2015.10.012.

52. Rhodes, D., and Hanson, A.D. (1993). Quaternary ammonium and tertiary sulfonium compounds in higher plants. Annual Review of Plant Physiology and Plant Molecular Biology *44*, 357–384. 10.1146/annurev.pp.44.060193.002041.

53. Stefels, J. (2000). Physiological aspects of the production and conversion of DMSP in marine algae and higher plants. Journal of Sea Research *43*, 183–197. 10.1016/S1385-1101(00)00030-7.

54. Bendif, E.M., Nevado, B., Wong, E.L.Y., Hagino, K., Probert, I., Young, J.R., Rickaby, R.E.M., and Filatov, D.A. (2019). Repeated species radiations in the recent evolution of the key marine phytoplankton lineage *Gephyrocapsa*. Nature Communications *10*, 4234. 10.1038/s41467-019-12169-7.

55. Bramucci, A.R., Labeeuw, L., Orata, F.D., Ryan, E.M., Malmstrom, R.R., and Case, R.J. (2018). The bacterial symbiont *Phaeobacter inhibens* shapes the life history of Its algal host *Emiliania huxleyi*. Frontiers in Marine Science *5*. 10.3389/fmars.2018.00188.

56. Kanehisa, M., and Goto, S. (2000). KEGG: Kyoto Encyclopedia of Genes and Genomes. Nucleic Acids Research *28*, 27–30. 10.1093/nar/28.1.27.

57. Howard, E.C., Henriksen, J.R., Buchan, A., Reisch, C.R., Bürgmann, H., Welsh, R., Ye, W., González, J.M., Mace, K., Joye, S.B., et al. (2006). Bacterial taxa that limit sulfur flux from the ocean. Science *314*, 649–652. 10.1126/science.1130657.

58. Curson, A.R.J., Todd, J.D., Sullivan, M.J., and Johnston, A.W.B. (2011). Catabolism of dimethylsulphoniopropionate: microorganisms, enzymes and genes. Nat Rev Microbiol *9*, 849–859. 10.1038/nrmicro2653.

59. Reisch, C.R., Stoudemayer, M.J., Varaljay, V.A., Amster, I.J., Moran, M.A., and Whitman, W.B. (2011). Novel pathway for assimilation of dimethylsulphoniopropionate widespread in marine bacteria. Nature *473*, 208–211. 10.1038/nature10078.

60. Johnston, A.W., Green, R.T., and Todd, J.D. (2016). Enzymatic breakage of dimethylsulfoniopropionate—a signature molecule for life at sea. Current Opinion in Chemical Biology *31*, 58–65. 10.1016/j.cbpa.2016.01.011.

61. Zhang, X.-H., Liu, J., Liu, J., Yang, G., Xue, C.-X., Curson, A.R.J., and Todd, J.D. (2019). Biogenic production of DMSP and its degradation to DMS—their roles in the global sulfur cycle. Science China Life Sciences *62*, 1296–1319. 10.1007/s11427-018-9524-y.

62. Hondorp, E.R., and Matthews, R.G. (2006). Methionine. EcoSal Plus *2*. 10.1128/ecosalplus.3.6.1.7.

63. Reisch, C.R., Moran, M.A., and Whitman, W.B. (2008). Dimethylsulfoniopropionate-dependent demethylase (DmdA) from *Pelagibacter ubique* and *Silicibacter pomeroyi*. Journal of Bacteriology *190*, 8018–8024. 10.1128/JB.00770-08.

64. Gao, C., Fernandez, V.I., Lee, K.S., Fenizia, S., Pohnert, G., Seymour, J.R., Raina, J.-B., and Stocker, R. (2020). Single-cell bacterial transcription measurements reveal the importance of dimethylsulfoniopropionate (DMSP) hotspots in ocean sulfur cycling. Nature Communications *11*, 1942. 10.1038/s41467-020-15693-z.

65. Neidhardt, F.C., Ingraham, J.L., and Schaechter, M. (1990). Physiology of the bacterial cell: a molecular approach (Springer).

66. Feist, A.M., Henry, C.S., Reed, J.L., Krummenacker, M., Joyce, A.R., Karp, P.D., Broadbelt, L.J., Hatzimanikatis, V., and Palsson, B.Ø. (2007). A genome-scale metabolic reconstruction for *Escherichia coli* K-12 MG1655 that accounts for 1260 ORFs and thermodynamic information. Molecular Systems Biology *3*, 121. 10.1038/msb4100155.

67. Miller-Fleming, L., Olin-Sandoval, V., Campbell, K., and Ralser, M. (2015). Remaining mysteries of molecular biology: the role of polyamines in the cell. Journal of Molecular Biology *427*, 3389–3406. 10.1016/j.jmb.2015.06.020.

68. Price, M.N., Zane, G.M., Kuehl, J.V., Melnyk, R.A., Wall, J.D., Deutschbauer, A.M., and Arkin, A.P. (2018). Filling gaps in bacterial amino acid biosynthesis pathways with high-throughput genetics. PLOS Genetics *14*, e1007147. 10.1371/journal.pgen.1007147.

69. Dickschat, J.S., Rabe, P., and Citron, C.A. (2015). The chemical biology of dimethylsulfoniopropionate. Org. Biomol. Chem. *13*, 1954–1968. 10.1039/C4OB02407A.

70. Weissbach, H., and Brot, N. (1991). Regulation of methionine synthesis in *Escherichia coli*. Molecular Microbiology *5*, 1593–1597. 10.1111/j.1365-2958.1991.tb01905.x.

71. Garrow, T.A. (1996). Purification, kinetic properties, and cDNA cloning of mammalian betaine-homocysteine methyltransferase. Journal of Biological Chemistry *271*, 22831–22838. 10.1074/jbc.271.37.22831.

72. Evans, J.C., Huddler, D.P., Jiracek, J., Castro, C., Millian, N.S., Garrow, T.A., and Ludwig, M.L. (2002). Betaine-homocysteine methyltransferase: zinc in a distorted barrel. Structure *10*, 1159–1171. 10.1016/S0969-2126(02)00796-7.

73. Barra, L., Fontenelle, C., Ermel, G., Trautwetter, A., Walker, G.C., and Blanco, C. (2006). Interrelations between glycine betaine catabolism and methionine biosynthesis in *Sinorhizobium meliloti* strain 102F34. Journal of Bacteriology *188*, 7195–7204. 10.1128/JB.00208-06.

74. Thanbichler, M., Neuhierl, B., and Böck, A. (1999). *S*-methylmethionine metabolism in *Escherichia coli*. J Bacteriol *181*, 662–665. 10.1128/JB.181.2.662-665.1999.

75. Li, K., Li, G., Bradbury, L.M.T., Hanson, A.D., and Bruner, S.D. (2016). Crystal structure of the homocysteine methyltransferase MmuM from *Escherichia coli*. Biochemical Journal *473*, 277–284. 10.1042/BJ20150980.

76. Szegedi, S.S., Castro, C.C., Koutmos, M., and Garrow, T.A. (2008). Betaine-homocysteine *S*-methyltransferase-2 is an *S*-methylmethionine-homocysteine methyltransferase. Journal of Biological Chemistry *283*, 8939–8945. 10.1074/jbc.M710449200.

77. Lee, M.B., Blunt, J.W., Lever, M., and George, P.M. (2004). A nuclear-magnetic-resonance-based assay for betaine–homocysteine methyltransferase activity. Analytical Biochemistry *330*, 199–205. 10.1016/j.ab.2004.03.069.

78. Mulligan, J.D., Laurie, T.J., and Garrow, T.A. (1998). An assay for betaine-homocysteine methyltransferase activity based on the microbiological detection of methionine. The Journal of Nutritional Biochemistry *9*, 351–354. 10.1016/S0955-2863(98)00025-4.

79. Pejchal, R., and Ludwig, M.L. (2004). Cobalamin-independent methionine synthase (MetE): a face-to-face double barrel that evolved by gene duplication. PLOS Biology *3*, e31. 10.1371/journal.pbio.0030031.

80. Husna, A.U., Wang, N., Cobbold, S.A., Newton, H.J., Hocking, D.M., Wilksch, J.J., Scott, T.A., Davies, M.R., Hinton, J.C., Tree, J.J., et al. (2018). Methionine biosynthesis and transport are functionally redundant for the growth and virulence of *Salmonella Typhimurium*. Journal of Biological Chemistry *293*, 9506–9519. 10.1074/jbc.RA118.002592.

81. Cruz, A.T., Cazacu, A.C., and Allen, C.H. (2007). *Pantoea agglomerans*, a plant pathogen causing human disease. Journal of Clinical Microbiology *45*, 1989–1992. 10.1128/JCM.00632-07.

82. Esposito, S., Miconi, F., Molinari, D., Savarese, E., Celi, F., Marchese, L., Valloscuro, S., Miconi, G., and Principi, N. (2019). What is the role of *Ewingella americana* in humans? A case report in a healthy 4-year-old girl. BMC Infectious Diseases *19*, 386. 10.1186/s12879-019-4021-4.

83. Bourgis, F., Roje, S., Nuccio, M.L., Fisher, D.B., Tarczynski, M.C., Li, C., Herschbach, C., Rennenberg, H., Pimenta, M.J., Shen, T.-L., et al. (1999). *S*-methylmethionine plays a major role in phloem sulfur transport and is synthesized by a novel type of methyltransferase. The Plant Cell *11*, 1485–1497. 10.1105/tpc.11.8.1485.

84. Chambers, S.T., Kunin, C.M., Miller, D., and Hamada, A. (1987). Dimethylthetin can substitute for glycine betaine as an osmoprotectant molecule for *Escherichia coli*. Journal of Bacteriology *169*, 4845–4847. 10.1128/jb.169.10.4845-4847.1987.

85. Diaz, M.R., Visscher, P.T., and Taylor, B.F. (1992). Metabolism of dimethylsulfoniopropionate and glycine betaine by a marine bacterium. FEMS Microbiology Letters *96*, 61–65. 10.1111/j.1574-6968.1992.tb05394.x.

86. Uguen, P., Hamelin, J., Le Pennec, J.-P., and Blanco, C. (1999). Influence of osmolarity and the presence of an osmoprotectant on *Lactococcus lactis* growth and bacteriocin production. Applied and Environmental Microbiology *65*, 291–293. 10.1128/AEM.65.1.291-293.1999.

87. Smits, S.H.J., Höing, M., Lecher, J., Jebbar, M., Schmitt, L., and Bremer, E. (2008). The compatible-solute-binding protein OpuAC from *Bacillus subtilis*: ligand binding, site-directed mutagenesis, and crystallographic studies. Journal of Bacteriology *190*, 5663–5671. 10.1128/JB.00346-08.

88. Bashir, A., Hoffmann, T., Smits, S.H.J., and Bremer, E. (2014). Dimethylglycine provides salt and temperature stress protection to *Bacillus subtilis*. Applied and Environmental Microbiology *80*, 2773–2785. 10.1128/AEM.00078-14.

89. Cosquer, A., Pichereau, V., Pocard, J.-A., Minet, J., Cormier, M., and Bernard, T. (1999). Nanomolar levels of dimethylsulfoniopropionate, dimethylsulfonioacetate, and glycine betaine are sufficient to confer osmoprotection to *Escherichia coli*. Applied and Environmental Microbiology *65*, 3304–3311. 10.1128/AEM.65.8.3304-3311.1999.

90. Gregory, G.J., Boas, K.E., and Boyd, E.F. (2021). The organosulfur compound dimethylsulfoniopropionate (DMSP) is utilized as an osmoprotectant by *Vibrio* species. Appl Environ Microbiol *87*, e02235-20. 10.1128/AEM.02235-20.

91. Welsh, D.T. (2000). Ecological significance of compatible solute accumulation by micro-organisms: from single cells to global climate. FEMS Microbiology Reviews *24*, 263–290. 10.1111/j.1574-6976.2000.tb00542.x.

92. Brill, J., Hoffmann, T., Bleisteiner, M., and Bremer, E. (2011). Osmotically controlled synthesis of the compatible solute proline is critical for cellular defense of *Bacillus subtilis* against high osmolarity. Journal of Bacteriology *193*, 5335–5346. 10.1128/JB.05490-11.

93. Ignatova, Z., and Gierasch, L.M. (2006). Inhibition of protein aggregation *in vitro* and *in vivo* by a natural osmoprotectant. Proceedings of the National Academy of Sciences *103*, 13357–13361. 10.1073/pnas.0603772103.

94. Liang, X., Zhang, L., Natarajan, S.K., and Becker, D.F. (2013). Proline mechanisms of stress survival. Antioxidants & Redox Signaling *19*, 998–1011. 10.1089/ars.2012.5074.

95. Wirth, J.S., Wang, T., Huang, Q., White, R.H., and Whitman, W.B. (2020). Dimethylsulfoniopropionate sulfur and methyl carbon assimilation in *Ruegeria* species. mBio *11*, e00329-20. 10.1128/mBio.00329-20.

96. Kiene, R.P., and Williams, L.P.H. (1998). Glycine betaine uptake, retention, and degradation by microorganisms in seawater. Limnology and Oceanography *43*, 1592–1603. 10.4319/lo.1998.43.7.1592.

97. Kiene, R.P., Linn, L.J., González, J., Moran, M.A., and Bruton, J.A. (1999). Dimethylsulfoniopropionate and methanethiol are important precursors of methionine and protein-sulfur in marine bacterioplankton. Applied and Environmental Microbiology *65*, 4549–4558. 10.1128/AEM.65.10.4549-4558.1999.

98. Bolten, C.J. (2010). Towards methionine overproduction in *Corynebacterium glutamicum* - methanethiol and dimethyldisulfide as reduced sulfur sources. J. Microbiol. Biotechnol. *20*, 1196–1203. 10.4014/jmb.1002.02018.

99. Reisch, C.R., Crabb, W.M., Gifford, S.M., Teng, Q., Stoudemayer, M.J., Moran, M.A., and Whitman, W.B. (2013). Metabolism of dimethylsulphoniopropionate by *Ruegeria pomeroyi* DSS-3. Molecular Microbiology *89*, 774–791. 10.1111/mmi.12314.

100. Chistoserdova, L. (2015). Methylotrophs in natural habitats: current insights through metagenomics. Appl Microbiol Biotechnol *99*, 5763–5779. 10.1007/s00253-015-6713-z.

101. Boysen, A.K., Durham, B.P., Kumler, W., Key, R.S., Heal, K.R., Carlson, L.T., Groussman, R.D., Armbrust, E.V., and Ingalls, A.E. (2022). Glycine betaine uptake and metabolism in marine microbial communities. Environmental Microbiology *24*, 2380–2403. 10.1111/1462-2920.16020.

102. Ducker, G.S., and Rabinowitz, J.D. (2017). One-carbon metabolism in health and disease. Cell Metabolism *25*, 27–42. 10.1016/j.cmet.2016.08.009.

103. Shetty, S., and Varshney, U. (2021). Regulation of translation by one-carbon metabolism in bacteria and eukaryotic organelles. Journal of Biological Chemistry *296*, 100088. 10.1074/jbc.REV120.011985.

104. Stauffer, G.V. (2004). Regulation of serine, glycine, and one-carbon biosynthesis. EcoSal Plus *1*. 10.1128/ecosalplus.3.6.1.2.

105. Oliveira, P.H., and Fang, G. (2021). Conserved DNA methyltransferases: a window into fundamental mechanisms of epigenetic regulation in bacteria. Trends in Microbiology *29*, 28–40. 10.1016/j.tim.2020.04.007.

106. Höfer, K., and Jäschke, A. (2018). Epitranscriptomics: RNA modifications in bacteria and archaea. In Regulating with RNA in Bacteria and Archaea, pp. 399–420. 10.1128/9781683670247.ch23.

107. Murn, J., and Shi, Y. (2017). The winding path of protein methylation research: milestones and new frontiers. Nature Reviews Molecular Cell Biology *18*, 517–527. 10.1038/nrm.2017.35.

108. Mouammine, A., and Collier, J. (2018). The impact of DNA methylation in Alphaproteobacteria. Molecular Microbiology *110*, 1–10. 10.1111/mmi.14079.

109. Fustin, J.-M., Ye, S., Rakers, C., Kaneko, K., Fukumoto, K., Yamano, M., Versteven, M., Grünewald, E., Cargill, S.J., Tamai, T.K., et al. (2020). Methylation deficiency disrupts biological rhythms from bacteria to humans. Communications Biology *3*, 211. 10.1038/s42003-020-0942-0.

110. Salah Ud-Din, A.I.M., and Roujeinikova, A. (2017). Methyl-accepting chemotaxis proteins: a core sensing element in prokaryotes and archaea. Cellular and Molecular Life Sciences *74*, 3293–3303. 10.1007/s00018-017-2514-0.

111. Kikuchi, G., Motokawa, Y., Yoshida, T., and Hiraga, K. (2008). Glycine cleavage system: reaction mechanism, physiological significance, and hyperglycinemia. Proceedings of the Japan Academy, Series B *84*, 246–263. 10.2183/pjab.84.246.

112. Sun, J., Steindler, L., Thrash, J.C., Halsey, K.H., Smith, D.P., Carter, A.E., Landry, Z.C., and Giovannoni, S.J. (2011). One carbon metabolism in SAR11 pelagic marine bacteria. PLOS ONE *6*, e23973. 10.1371/journal.pone.0023973.

113. Lidbury, I.D., Murrell, J.C., and Chen, Y. (2015). Trimethylamine and trimethylamine *N*-oxide are supplementary energy sources for a marine heterotrophic bacterium: implications for marine carbon and nitrogen cycling. ISME J *9*, 760–769. 10.1038/ismej.2014.149.

114. Kotte, O., Volkmer, B., Radzikowski, J.L., and Heinemann, M. (2014). Phenotypic bistability in *Escherichia coli*'s central carbon metabolism. Molecular Systems Biology *10*, 736. 10.15252/msb.20135022.

115. Balaban, N.Q., Merrin, J., Chait, R., Kowalik, L., and Leibler, S. (2004). Bacterial persistence as a phenotypic switch. Science *305*, 1622–1625. 10.1126/science.1099390.

116. Meinnel, T., Mechulam, Y., and Blanquet, S. (1993). Methionine as translation start signal: a review of the enzymes of the pathway in *Escherichia coli*. Biochimie *75*, 1061–1075. 10.1016/0300-9084(93)90005-D.

117. Guillon, J.M., Mechulam, Y., Schmitter, J.M., Blanquet, S., and Fayat, G. (1992). Disruption of the gene for Met-tRNA (fMet) formyltransferase severely impairs growth of *Escherichia coli*. Journal of Bacteriology *174*, 4294–4301. 10.1128/jb.174.13.4294-4301.1992.

118. Vanunu, M., Lang, Z., and Barkan, D. (2017). The gene *fmt*, encoding tRNAfMet-formyl transferase, is essential for normal growth of *M. bovis*, but not for viability. Scientific Reports *7*, 15161. 10.1038/s41598-017-15618-9.

119. Fridman, O., Goldberg, A., Ronin, I., Shoresh, N., and Balaban, N.Q. (2014). Optimization of lag time underlies antibiotic tolerance in evolved bacterial populations. Nature *513*, 418–421. 10.1038/nature13469.

120. Kumar, D., and Gomes, J. (2005). Methionine production by fermentation. Biotechnology Advances *23*, 41–61. 10.1016/j.biotechadv.2004.08.005.

121. Finkelstein, J.D. (1990). Methionine metabolism in mammals. The Journal of Nutritional Biochemistry *1*, 228–237. 10.1016/0955-2863(90)90070-2.

122. Froese, D.S., Fowler, B., and Baumgartner, M.R. (2019). Vitamin B12, folate, and the methionine remethylation cycle—biochemistry, pathways, and regulation. Journal of Inherited Metabolic Disease *42*, 673–685. 10.1002/jimd.12009.

123. Lee, L.-W., Ravel, J.M., and Shive, W. (1966). Multimetabolite control of a biosynthetic pathway by sequential metabolites. Journal of Biological Chemistry *241*, 5479–5480. 10.1016/S0021-9258(18)96455-0.

124. Roe, A.J., O'Byrne, C., McLaggan, D., and Booth, I.R. (2002). Inhibition of *Escherichia coli* growth by acetic acid: a problem with methionine biosynthesis and homocysteine toxicity. Microbiology *148*, 2215–2222. 10.1099/00221287-148-7-2215.

125. Schink, S.J., Gough, Z., Biselli, E., Huiman, M.G., Chang, Y.-F., Basan, M., and Gerland, U. (2022). MetA is a "thermal fuse" that inhibits growth and protects *Escherichia coli* at elevated temperatures. Cell Reports *40*, 111290. 10.1016/j.celrep.2022.111290.

126. Barak-Gavish, N., Dassa, B., Kuhlisch, C., Nussbaum, I., Brandis, A., Rosenberg, G., Avraham, R., and Vardi, A. (2023). Bacterial lifestyle switch in response to algal metabolites. eLife *12*, e84400. 10.7554/eLife.84400.

127. Wei, Y., and Newman, E.B. (2002). Studies on the role of the *metK* gene product of *Escherichia coli* K-12. Molecular Microbiology *43*, 1651–1656. 10.1046/j.1365-2958.2002.02856.x.

128. Igarashi, K., and Kashiwagi, K. (2018). Effects of polyamines on protein synthesis and growth of *Escherichia coli*. Journal of Biological Chemistry *293*, 18702–18709. 10.1074/jbc.TM118.003465.

129. Cunningham-Rundles, S., and Maas, W.K. (1975). Isolation, characterization, and mapping of *Escherichia coli* mutants blocked in the synthesis of ornithine decarboxylase. Journal of Bacteriology *124*, 791–799. 10.1128/jb.124.2.791-799.1975.

130. Hafner, E.W., Tabor, C.W., and Tabor, H. (1979). Mutants of *Escherichia coli* that do not contain 1,4-diaminobutane (putrescine) or spermidine. Journal of Biological Chemistry *254*, 12419–12426. 10.1016/S0021-9258(19)86331-7.

131. Tabor, H., Hafner, E.W., and Tabor, C.W. (1980). Construction of an *Escherichia coli* strain unable to synthesize putrescine, spermidine, or cadaverine: characterization of two genes controlling lysine decarboxylase. Journal of Bacteriology *144*, 952–956. 10.1128/jb.144.3.952-956.1980.

132. Yohannes, E., Thurber, A.E., Wilks, J.C., Tate, D.P., and Slonczewski, J.L. (2005). Polyamine stress at high pH in *Escherichia coli* K-12. BMC Microbiology *5*, 59. 10.1186/1471-2180-5-59.

133. Chattopadhyay, M.K., Tabor, C.W., and Tabor, H. (2003). Polyamines protect *Escherichia coli* cells from the toxic effect of oxygen. Proceedings of the National Academy of Sciences *100*, 2261–2265. 10.1073/pnas.2627990100.

134. Tkachenko, A.G., Akhova, A.V., Shumkov, M.S., and Nesterova, L.Y. (2012). Polyamines reduce oxidative stress in *Escherichia coli* cells exposed to bactericidal antibiotics. Research in Microbiology *163*, 83–91. 10.1016/j.resmic.2011.10.009.

135. Jung, I.L., Oh, T.J., and Kim, I.G. (2003). Abnormal growth of polyamine-deficient *Escherichia coli* mutant is partially caused by oxidative stress-induced damage. Archives of Biochemistry and Biophysics *418*, 125–132. 10.1016/j.abb.2003.08.003.

136. Bower, J.M., and Mulvey, M.A. (2006). Polyamine-mediated resistance of uropathogenic *Escherichia coli* to nitrosative stress. J Bacteriol *188*, 928–933. 10.1128/JB.188.3.928-933.2006.

137. Hetrick, B., Khade, P.K., Lee, K., Stephen, J., Thomas, A., and Joseph, S. (2010). Polyamines accelerate codon recognition by transfer RNAs on the ribosome. Biochemistry *49*, 7179–7189. 10.1021/bi1009776.

138. Pin, C., Rolfe, M.D., Muñoz-Cuevas, M., Hinton, J.C., Peck, M.W., Walton, N.J., and Baranyi, J. (2009). Network analysis of the transcriptional pattern of young and old cells of *Escherichia coli* during lag phase. BMC Systems Biology *3*, 108. 10.1186/1752-0509-3-108.

139. Kolter, R., Balaban, N., and Julou, T. (2022). Bacteria grow swiftly and live thriftily. Current Biology *32*, R599–R605. 10.1016/j.cub.2022.05.005.

140. Despotović, D., Aharon, E., Trofimyuk, O., Dubovetskyi, A., Cherukuri, K.P., Ashani, Y., Eliason, O., Sperfeld, M., Leader, H., Castelli, A., et al. (2022). Utilization of diverse organophosphorus pollutants by marine bacteria. Proceedings of the National Academy of Sciences *119*, e2203604119. 10.1073/pnas.2203604119.

141. Kehe, J., Ortiz, A., Kulesa, A., Gore, J., Blainey, P.C., and Friedman, J. (2021). Positive interactions are common among culturable bacteria. Science Advances *7*, eabi7159. 10.1126/sciadv.abi7159.

142. Sperfeld, M., Yahalomi, D., and Segev, E. (2022). Resolving the microalgal gene landscape at the strain level: a novel hybrid transcriptome of *Emiliania huxleyi* CCMP3266. Applied and Environmental Microbiology *88*, e01418-21. 10.1128/AEM.01418-21.

143. O'Leary, N.A., Wright, M.W., Brister, J.R., Ciufo, S., Haddad, D., McVeigh, R., Rajput, B., Robbertse, B., Smith-White, B., Ako-Adjei, D., et al. (2016). Reference sequence (RefSeq) database at NCBI: current status, taxonomic expansion, and functional annotation. Nucleic Acids Research *44*, D733–D745. 10.1093/nar/gkv1189.

144. Karp, P.D., Billington, R., Caspi, R., Fulcher, C.A., Latendresse, M., Kothari, A., Keseler, I.M., Krummenacker, M., Midford, P.E., Ong, Q., et al. (2019). The BioCyc collection of microbial genomes and metabolic pathways. Briefings in Bioinformatics *20*, 1085–1093. 10.1093/bib/bbx085.

145. Kovach, M.E., Elzer, P.H., Steven Hill, D., Robertson, G.T., Farris, M.A., Roop, R.M., and Peterson, K.M. (1995). Four new derivatives of the broad-host-range cloning vector pBBR1MCS, carrying different antibiotic-resistance cassettes. Gene *166*, 175–176. 10.1016/0378-1119(95)00584-1.

146. Aronesty, E. (2013). Comparison of sequencing utility programs. The Open Bioinformatics Journal *7*. 10.2174/1875036201307010001.

147. Martin, M. (2011). Cutadapt removes adapter sequences from high-throughput sequencing reads. EMBnet.journal *17*, 10–12. 10.14806/ej.17.1.200.

148. Dobin, A., Davis, C.A., Schlesinger, F., Drenkow, J., Zaleski, C., Jha, S., Batut, P., Chaisson, M., and Gingeras, T.R. (2013). STAR: ultrafast universal RNA-seq aligner. Bioinformatics *29*, 15–21. 10.1093/bioinformatics/bts635.

149. Liao, Y., Smyth, G.K., and Shi, W. (2014). featureCounts: An efficient general purpose program for assigning sequence reads to genomic features. Bioinformatics *30*, 923–930. 10.1093/bioinformatics/btt656.

150. Love, M.I., Huber, W., and Anders, S. (2014). Moderated estimation of fold change and dispersion for RNA-seq data with DESeq2. Genome Biology *15*, 550. 10.1186/s13059-014-0550-8.

151. R Core Team (2022). R: A Language and Environment for Statistical Computing. R Foundation for Statistical Computing, Vienna, Austria. URL https://www.R-project.org/.

152. Wickham, H. (2016). ggplot2: Elegant Graphics for Data Analysis 2nd ed. 2016. (Springer International Publishing : Imprint: Springer) 10.1007/978-3-319-24277-4.

153. Sprouffske, K., and Wagner, A. (2016). Growthcurver: an R package for obtaining interpretable metrics from microbial growth curves. BMC Bioinformatics *17*, 172. 10.1186/s12859-016-1016-7.

154. Hothorn, T., Bretz, F., and Westfall, P. (2008). Simultaneous inference in general parametric models. Biometrical Journal *50*, 346–363. 10.1002/bimj.200810425.

155. Goyet, C., and Poisson, A. (1989). New determination of carbonic acid dissociation constants in seawater as a function of temperature and salinity. Deep Sea Research Part A. Oceanographic Research Papers *36*, 1635–1654. 10.1016/0198-0149(89)90064-2.

156. Beiralas, R., and Segev, E. (2023). *Sulfitobacter_pontiacus*_isolate_*huxleyi*1516. 10.5281/zenodo.7520022.

157. Avraham, R., Haseley, N., Fan, A., Bloom-Ackermann, Z., Livny, J., and Hung, D.T. (2016). A highly multiplexed and sensitive RNA-seq protocol for simultaneous analysis of host and pathogen transcriptomes. Nature Protocols *11*, 1477–1491. 10.1038/nprot.2016.090.

158. Anders, S., and Huber, W. (2010). Differential expression analysis for sequence count data. Genome Biology *11*, R106. 10.1186/gb-2010-11-10-r106.

159. Zhu, A., Ibrahim, J.G., and Love, M.I. (2019). Heavy-tailed prior distributions for sequence count data: removing the noise and preserving large differences. Bioinformatics *35*, 2084–2092. 10.1093/bioinformatics/bty895.

160. The UniProt Consortium (2023). UniProt: the universal protein knowledgebase in 2023. Nucleic Acids Research *51*, D523–D531. 10.1093/nar/gkac1052.

161. Paysan-Lafosse, T., Blum, M., Chuguransky, S., Grego, T., Pinto, B.L., Salazar, G.A., Bileschi, M.L., Bork, P., Bridge, A., Colwell, L., et al. (2023). InterPro in 2022. Nucleic Acids Research *51*, D418–D427. 10.1093/nar/gkac993.

162. Chen, Y. (2012). Comparative genomics of methylated amine utilization by marine *Roseobacter* clade bacteria and development of functional gene markers (*tmm*, *gmaS*). Environmental Microbiology *14*, 2308–2322. 10.1111/j.1462-2920.2012.02765.x.

163. Chistoserdova, L. (2011). Modularity of methylotrophy, revisited. Environmental Microbiology *13*, 2603–2622. 10.1111/j.1462-2920.2011.02464.x.

164. Altschul, S.F., Gish, W., Miller, W., Myers, E.W., and Lipman, D.J. (1990). Basic local alignment search tool. Journal of Molecular Biology *215*, 403–410. 10.1016/S0022-2836(05)80360-2.

165. Sklodowska, K., and Jakiela, S. (2017). Enhancement of bacterial growth with the help of immiscible oxygenated oils. RSC Adv. *7*, 40990–40995. 10.1039/C7RA07095K.

166. Peleg, Y., and Unger, T. (2014). Application of the Restriction-Free (RF) cloning for multicomponents assembly. In DNA Cloning and Assembly Methods Methods in Molecular Biology., S. Valla and R. Lale, eds. (Humana Press), pp. 73–87. 10.1007/978-1-62703-764-8_6.

167. Dower, W.J., Miller, J.F., and Ragsdale, C.W. (1988). High efficiency transformation of *E. coli* by high voltage electroporation. Nucleic Acids Research *16*, 6127–6145. 10.1093/nar/16.13.6127.

168. Geiger, O., López-Lara, I.M., and Sohlenkamp, C. (2013). Phosphatidylcholine biosynthesis and function in bacteria. Biochimica et Biophysica Acta (BBA) - Molecular and Cell Biology of Lipids *1831*, 503–513. 10.1016/j.bbalip.2012.08.009.

169. Martens, T., Heidorn, T., Pukall, R., Simon, M., Tindall, B.J., and Brinkhoff, T. (2006). Reclassification of *Roseobacter gallaeciensis* Ruiz-Ponte *et al.* 1998 as *Phaeobacter gallaeciensis* gen. nov., comb. nov., description of *Phaeobacter inhibens* sp. nov., reclassification of *Ruegeria algicola* (Lafay *et al.* 1995) Uchino *et al.* 1999 as *Marinovum algicola* gen. nov., comb. nov., and emended descriptions of the genera *Roseobacter, Ruegeria* and *Leisingera*. International Journal of Systematic and Evolutionary Microbiology *56*, 1293–1304. 10.1099/ijs.0.63724-0.

170. Bullock, H.A., Reisch, C.R., Burns, A.S., Moran, M.A., and Whitman, W.B. (2014). Regulatory and functional diversity of methylmercaptopropionate coenzyme A ligases from the dimethylsulfoniopropionate demethylation pathway in *Ruegeria pomeroyi* DSS-3 and other proteobacteria. Journal of Bacteriology *196*, 1275–1285. 10.1128/JB.00026-14.

171. Dickschat, J.S., Zell, C., and Brock, N.L. (2010). Pathways and substrate specificity of DMSP catabolism in marine bacteria of the Roseobacter clade. ChemBioChem *11*, 417–425. 10.1002/cbic.200900668.

172. Malitsky, S., Ziv, C., Rosenwasser, S., Zheng, S., Schatz, D., Porat, Z., Ben-Dor, S., Aharoni, A., and Vardi, A. (2016). Viral infection of the marine alga *Emiliania huxleyi* triggers lipidome remodeling and induces the production of highly saturated triacylglycerol. New Phytologist *210*, 88–96. 10.1111/nph.13852.

173. Zheng, L., Cardaci, S., Jerby, L., MacKenzie, E.D., Sciacovelli, M., Johnson, T.I., Gaude, E., King, A., Leach, J.D.G., Edrada-Ebel, R., et al. (2015). Fumarate induces redox-dependent senescence by modifying glutathione metabolism. Nat Commun *6*, 6001. 10.1038/ncomms7001.

174. Waditee, R., and Incharoensakdi, A. (2001). Purification and kinetic properties of betaine-homocysteine methyltransferase from *Aphanothece halophytica*. Curr Microbiol *43*, 107–111. 10.1007/s002840010270.

175. Smith, L.T., Pocard, J.A., Bernard, T., and Le Rudulier, D. (1988). Osmotic control of glycine betaine biosynthesis and degradation in *Rhizobium meliloti*. Journal of Bacteriology *170*, 3142–3149. 10.1128/jb.170.7.3142-3149.1988.

176. Quan, J., and Tian, J. (2009). Circular polymerase extension cloning of complex gene libraries and pathways. PLOS ONE *4*, e6441. 10.1371/journal.pone.0006441.

177. Ranocha, P., Bourgis, F., Ziemak, M.J., Rhodes, D., Gage, D.A., and Hanson, A.D. (2000). Characterization and functional expression of cDNAs encoding methionine-sensitive and-insensitive homocysteine *S*-methyltransferases from *Arabidopsis*. Journal of Biological Chemistry *275*, 15962–15968. 10.1074/jbc.M001116200.